

Resource Allocation for Cross-Layer Utility Maximization in Wireless Networks

Pradeep Chathuranga Weeraddana, *Student Member, IEEE*, Marian Codreanu, *Member, IEEE*,
Matti Latva-aho, *Senior Member, IEEE*, and Anthony Ephremides, *Fellow, IEEE*

Abstract—The cross-layer utility maximization problem, which is subject to stability constraints for a multicommodity wireless network where all links share the same number of orthogonal channels, is considered in this paper. We assume a time-slotted network, where the channel gains randomly change from one slot to another. The optimal cross-layer network control policy can be decomposed into the following three subproblems: 1) *flow control*; 2) *next-hop routing and in-node scheduling*; and 3) *power and rate control*, which is also known as *resource allocation* (RA). These subproblems span the layers from the physical layer to the transport layer. In every time slot, a network controller decides the amount of each commodity data admitted to the network layer, schedules different commodities over the network's links, and controls the power and rate allocated to every link in every channel. To fully exploit the available multichannel diversity, we consider the general case, where multiple links can be activated in the same channel during the same time slot, and the interference is controlled solely through power and rate control. Unfortunately, the RA subproblem is not yet amenable to a convex formulation, and in fact, it is NP-hard. The main contribution of this paper is to develop efficient RA algorithms for multicommodity multichannel wireless networks by applying complementary geometric programming and homotopy methods to analyze the quantitative impact of gains that can be achieved at the network layer in terms of end-to-end rates and network congestion by incorporating different RA algorithms. Although the global optimality of the solution cannot be guaranteed, the numerical results show that the proposed algorithms perform close to the (exponentially complex) optimal solution methods. Moreover, they efficiently exploit the available multichannel diversity, which provides significant gains at the network layer in terms of end-to-end rates and network congestion. In addition, the assessment of the improvement in performance due to the use of multiuser detectors at the receivers is provided.

Index Terms—Backpressure, complementary geometric programming (CGP), cross-layer optimization, fairness, homotopy methods, multichannel diversity, network (NW)-layer capacity region, network utility maximization (NUM), resource allocation (RA), signomial programming (SP).

Manuscript received August 17, 2010; revised January 28, 2011 and April 8, 2011; accepted April 19, 2011. Date of publication May 27, 2011; date of current version July 18, 2011. This work was supported in part by the Finnish Funding Agency for Technology and Innovation, the Academy of Finland, Nokia, Nokia Siemens Networks, Elektrobitt, the Graduate School in Electronics, Telecommunications and Automation Foundations, Nokia Foundation, the National Science Foundation under Grant CCF0728966, and the U.S. Army Research Office under Grant W911NF-08-1-0238. The review of this paper was coordinated by Prof. B. Hamdaoui.

P. C. Weeraddana, M. Codreanu, and M. Latva-aho are with the Centre for Wireless Communications, Department of Electrical Engineering, University of Oulu, 90014 Oulu, Finland (e-mail: chathu@ee.oulu.fi; codreanu@ee.oulu.fi; matti.latva-aho@ee.oulu.fi).

A. Ephremides is with the University of Maryland, College Park, MD 20742 USA (e-mail: etony@ece.umd.edu).

Color versions of one or more of the figures in this paper are available online at <http://ieeexplore.ieee.org>.

Digital Object Identifier 10.1109/TVT.2011.2157544

I. INTRODUCTION

IN THE late 1990s, Kelly *et al.* [1], [2] introduced the concept of network utility maximization (NUM) for fairness control in wireline networks (NWs). It was shown that maximizing the sum rate under the fairness constraint is equivalent to maximizing certain NW utility functions, and different NW utility functions can be mapped to different fairness criteria. In [3]–[7], Lin and Shroff, Neely *et al.*, Stolyar, and Eryilmaz and Srikant extended Kelly's NUM framework to cover certain aspects of wireless NWs. It has been shown that an optimal cross-layer control policy, which achieves data rates that are arbitrarily close to the optimal operating point, can be decomposed into three subproblems that are normally associated with different NW layers. In particular, *flow control* resides at the transport layer, *routing and in-node scheduling*¹ resides at the NW layer, and *resource allocation* (RA) is usually associated with the medium access control (MAC) and physical (PHY) layers [4].

The first two subproblems are convex optimization problems and can relatively easily be solved. Under reasonably mild assumptions, the RA subproblem can be cast as a general weighted sum-rate maximization over the instantaneous achievable rate region [4], [8]–[11]. The weights of the links are given by the differential backlogs, and the policy resembles the well-known *backpressure algorithm* introduced by Tassiulas and Ephremides in [12], [13] and further extended in [9], [14], and [15] to dynamic NWs with power control. In the case of wireless NWs, the achievable rates on the links are interdependent due to interference, i.e., the achievable rate of a particular link depends on the powers allocated to all other links. This coupling makes the RA subproblem a difficult nonconvex optimization problem [16]. In fact, it is NP-hard [17]. Roughly speaking, this means that, by employing global optimization approaches [18]–[20], the worst-case computational complexity for solving the RA subproblem more than polynomially increases with the number of variables. Therefore, the RA subproblem appears to be a thorny problem in cross-layer utility maximization for wireless NWs, and certainly, it deserves efficient algorithms that, although suboptimal, perform well in practice. In this paper, we develop such RA algorithms for general wireless NWs by applying *homotopy methods* (or continuation methods) [21] together with complementary geometric programming (CGP) [22].

¹*In-node scheduling* refers to selecting the appropriate commodity, and it should not be confused with the links scheduling mechanism, which is handled by the RA subproblem [8].

A. Previous Work

In general cross-layer utility maximization problems, as proposed in [3]–[8], [10], and [11], the main focus resided in deriving optimal cross-layer control policies. Thus, very little attention has particularly been made on the PHY-layer RA subproblem. Optimal solution methods for solving similar problems based on exhaustive search or branch-and-bound techniques [18]–[20] have been proposed in [23]–[27]. Unfortunately, the computational complexity of these methods is prohibitively expensive, even for the offline optimization of moderate-size NWs. Several approximations have been proposed for the case when all links in the NW operate in certain signal-to-interference-plus-noise ratio (SINR) regions. For example, the assumption that the achievable rate is a linear function of the SINR (i.e., a low-SINR region) is widely used in ultrawideband systems [28]–[30]. In addition, [3], [31], and [32] provide solutions for the power and rate control in low-SINR regions. A high-SINR (HSINR) region is treated in [33]–[35]. However, at the optimal operating point, different links correspond to different SINR regions, which is usually the case for multihop NWs. Therefore, all aforementioned methods that are based on either the low-SINR or the HSINR assumption can fail to solve the general problem. One promising method is to cast the problem into a signomial programming (SP) formulation [36, Sec. 9] or into a CGP [22], where a suboptimal solution can quite efficiently be obtained.² Applications of SP and CGP solution methods have been demonstrated in various signal-processing and digital communications problems, e.g., [37]–[40]. Note that CGP cannot handle the self-interference problem that arises when a node simultaneously transmits and receives in the same frequency band. That is, for general multihop wireless NWs, the RA subproblem must also cope with the self-interference problem. Thus, only subsets of mutually exclusive links can simultaneously be activated to avoid the large self interference that is encountered if a node transmits and receives in the same frequency band [41]–[43]. Under such circumstances, SP/CGP cannot directly be applicable, even to obtain a better suboptimal solution, because the initialization of the algorithms plays a major role. If we still want to apply CGP for RA in general multihop NWs, all subsets of mutually exclusive links should be considered. This approach, in turn, induces a combinatorial nature for the RA subproblem. Nevertheless, SP/CGP solution methods are of crucial importance from both the theoretical and the practical perspectives because, in practice, we often encounter interference channels where neither low-SINR nor HSINR approximations are justifiable.

B. Our Contributions

In this paper, we develop efficient RA algorithms for multicommodity multichannel multihop wireless NWs by using *homotopy methods* [21] and CGP [22]. The proposed methods handle the self-interference problem such that the combinatorial nature of the problem is circumvented. Our RA problem formulation is fairly general, and it allows frequency reuse

²Note that we can readily convert an SP to a CGP and *vice versa* [37, Sec. 2.2.5].

by simultaneously activating multiple links in the same channel. Here, the interference is solely controlled through power control. Furthermore, our formulation allows the possibility of exploiting multichannel diversity through dynamic power allocation across the available channels. In addition, we quantitatively analyze the gains that can be achieved at upper layers in terms of end-to-end rates and NW congestion by incorporating different RA algorithms within Neely's cross-layer utility maximization framework [8], [9]. Recall that the RA subproblem is NP-hard and that we have to rely on exponentially complex global optimization techniques [18]–[20] to yield the optimal solution. Nevertheless, the numerical results show that the proposed RA algorithms perform close to global optimization methods. We further test our algorithms by applying them in large RA problems, where global optimization methods [23]–[27] cannot be used due to prohibitive computational complexity. Results show that the proposed algorithms can provide significant gains at the NW layer in terms of end-to-end rates and NW congestion by efficiently exploiting the available multichannel diversity. Finally, we consider different receiver capabilities and evaluate the effect of the use of multiuser (MU) detectors.

C. Organization and Notations

The rest of this paper is organized as follows. The system model and the problem formulation are presented in Section II. The proposed power control algorithms are presented in Section III. In Section IV, we consider the case of increased receiver capability. The numerical results are presented in Section V, and Section VI concludes this paper.

Notations are as given follows. All boldface lowercase and uppercase letters represent vectors and matrices, respectively, and script letters represent sets. The notation $[\mathbf{A}]_{p,q}$ denotes the (p, q) entry of the matrix \mathbf{A} , \mathbf{e}_i represents the i th standard unit vector, $\mathbb{R}_+^{m \times n}$ denotes the set of $m \times n$ real matrices with nonnegative entries, and \mathbb{R}_+^n denotes the cone of nonnegative n -dimensional real vectors (the n -dimensional nonnegative orthant). We use the notation $\{\cdot\}$ to describe the variables inside the brace either as a set or as a vector. $E\{\cdot\}$ denotes the statistical expectation, and $|\mathcal{X}|$ denotes the cardinality of the set \mathcal{X} . In addition, ∇f denotes the gradient of function f , and $\nabla^2 f$ is the second derivative (or Hessian matrix) of f . The superscript $(\cdot)^*$ is used to denote a solution of an optimization problem.

II. SYSTEM MODEL AND PROBLEM FORMULATION

A. NW Model

The wireless NW consists of a collection of nodes that can send, receive, and relay data across wireless links. The set of all nodes is denoted by \mathcal{N} , and we label the nodes with the integer values $n = 1, \dots, N$. A wireless link is represented as an ordered pair (i, j) of distinct nodes. The set of links is denoted by \mathcal{L} , and we label the links with the integer values $l = 1, \dots, L$. We define $tran(l)$ as the transmitter node of link l and $rec(l)$ as the receiver node of link l . The existence of a link $l \in \mathcal{L}$ implies that a direct transmission is possible from node $tran(l)$ to node $rec(l)$. We assume that each node

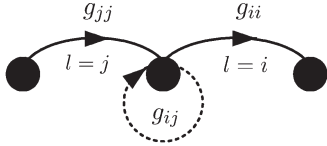


Fig. 1. Choosing the value of interference coefficients g_{ij} for $i \neq j$ and link power gains, i.e., g_{ii} and g_{jj} (the channel c and time t indices are omitted for clarity), where $\mathcal{A} = \{(i, j)\}$, $g_{ij} = 1$, $g_{ji} = |h_{ji}|^2$, $g_{ii} = |h_{ii}|^2$, and $g_{jj} = |h_{jj}|^2$.

can be equipped with multiple transceivers, i.e., any node can simultaneously transmit to or receive from multiple nodes. We define $\mathcal{O}(n)$ as the set of links that are outgoing from node n and $\mathcal{I}(n)$ as the set of links that are incoming to node n . Furthermore, we denote the set of transmitter nodes by \mathcal{T} and the set of receiver nodes by \mathcal{R} , i.e., $\mathcal{T} = \{n \in \mathcal{N} | \mathcal{O}(n) \neq \emptyset\}$ and $\mathcal{R} = \{n \in \mathcal{N} | \mathcal{I}(n) \neq \emptyset\}$.

The NW is assumed to operate in slotted time, with the slots normalized to integer values $t \in \{1, 2, 3, \dots\}$. All wireless links share a set \mathcal{C} of orthogonal channels, labeled with integers $c = 1, \dots, C$. When there are several channels that independently fade at any one time, there is a high probability that one of the channels will be strong. Thus, the main motivation for considering multiple channels is the exploitation of the diversity that results from unequal link behavior across a given wideband.

Let $h_{ijc}(t)$ denote the channel gain from the transmitter of link i to the receiver of link j in channel c during time slot t . We assume that $h_{ijc}(t)$ are constant for the duration of a time slot and are independent and identically distributed over the time slots, links, and channels. Let $g_{iic}(t)$ represent the power gain of link i in channel c during time slot t , i.e., $g_{iic}(t) = |h_{iic}(t)|^2$ (see Fig. 1). For any pair of *distinct* links $i \neq j$, we denote the interference coefficient from link i to link j in channel c by $g_{ijc}(t)$. For notational convenience, let \mathcal{A} denote the set of all link pairs (i, j) for which the transmitter of link i and the receiver of link j coincide, i.e., $\mathcal{A} = \{(i, j)_{i, j \in \mathcal{C}} | \text{tran}(i) = \text{rec}(j)\}$ (see Fig. 1). In other words, \mathcal{A} represents the set of all link pairs (i, j) for which $i \in \mathcal{O}(n)$ and $j \in \mathcal{I}(n)$ for some $n \in \mathcal{N}$. In the case of $(i, j) \in \mathcal{A}$, $g_{ijc}(t)$ represents the power gain within the same node from its transmitter to its receiver and is referred to as the self-interference gain (see Fig. 1). In particular, we let $g_{ijc}(t) = 1$ for all $(i, j) \in \mathcal{A}$ to model the very large self interference that will affect the incoming links of a node if it is simultaneously transmitted and received in the same channel. For all pairs (i, j) of *distinct* links such that $(i, j) \notin \mathcal{A}$, the term $g_{ijc}(t)$ represents the power of the interference signal at the receiver node of link j in channel c when one unit of power is allocated to the transmitter node of link i in the same channel, i.e., $g_{ijc}(t) = |h_{ijc}(t)|^2$ for all $(i, j) \notin \mathcal{A}$ (see Fig. 1). Note that, according to relative distances between the NW's nodes, $g_{ijc}(t)$ for all $(i, j) \in \mathcal{A}$ (i.e., the self-interference gains) can be several orders of magnitude larger than $g_{ijc}(t)$ for all $(i, j) \notin \mathcal{A}$ (i.e., the power gains of links and the interference coefficients of pairs of different links). The particular class of NW topologies, for which $\mathcal{A} = \emptyset$ (i.e., $\mathcal{T} \cap \mathcal{R} = \emptyset$), is referred to as *bipartite* NWs. On the other hand, the class of NW topologies, for which $\mathcal{A} \neq \emptyset$ (i.e., $\mathcal{T} \cap \mathcal{R} \neq \emptyset$), is referred to as *nonbipartite* NWs. Note that all multihop NWs are necessarily nonbipartite.

In every time slot, a NW controller decides the power and rates allocated to each link in every channel. We denote by $p_{lc}(t)$ the power that is allocated to each link l in channel c during time slot t . The power allocation is subject to a maximum power constraint $\sum_{c \in \mathcal{C}} \sum_{l \in \mathcal{O}(n)} p_{lc}(t) \leq p_n^{\max}$ for each node n .

We first consider the case where all receivers perform single-user detection³, and we assume that the achievable rate of link l during time slot t is given by

$$r_l(t) = \sum_{c=1}^C W_c \log \left(1 + \frac{g_{llc}(t)p_{lc}(t)}{N_l W_c + \sum_{j \neq l} g_{jlc}(t)p_{jc}(t)} \right), \quad (1)$$

where W_c represents the bandwidth of channel c , and N_l is the power spectral density of the noise at the receiver of link l . Note that, for any link l , interference at $\text{rec}(l)$ (i.e., the term $\sum_{j \neq l} g_{jlc}(t)p_{jc}(t)$) is created by self transmissions (i.e., $\sum_{j \in \mathcal{O}(\text{rec}(l))} g_{jlc}(t)p_{jc}(t)$), as well as by other node transmissions (i.e., $\sum_{j \in \mathcal{L} \setminus \{\mathcal{O}(\text{rec}(l)) \cup \{l\}\}} g_{jlc}(t)p_{jc}(t)$). To simplify the presentation, we assume in the rest of the paper that all channels have equal bandwidths and the noise power density is the same at all receivers⁴ (i.e., $W_c = W$ for all $c \in \mathcal{C}$ and $N_l = N_0$ for all $l \in \mathcal{L}$). Let $\sigma^2 = N_0 W$ denote the noise power, which is constant for all receivers in all channels. Furthermore, we denote by $\mathbf{P}(t) \in \mathbb{R}_+^{L \times C}$ the overall power allocation matrix, i.e., $p_{lc}(t) = [\mathbf{P}(t)]_{l,c}$. The use of the Shannon formula for the achievable rate in (1) is approximate in the case of finite-length packets and is used to avoid the complexity of rate-power dependence in practical modulation and coding schemes. This practice is common, but note that this approach is not strictly correct. However, as the packet length increases, it becomes asymptotically correct.

B. NUM and Problem Formulation

Exogenous data arrive at the source nodes, and they are delivered to the destination nodes over several (possibly multihop) paths. We identify the data by their destinations, i.e., all data with the same destination are considered a single commodity, regardless of the source. In fact, our formulation also permits the anycast case, in which each packet exits the NW as soon as any one of a particular destination set of nodes successfully receives the packet. We label the commodities with integers $s = 1, \dots, S$ ($S \leq N$), and the destination node of commodity s is denoted by d_s . For every node, we define $\mathcal{S}_n \subseteq \{1, \dots, S\}$ as the set of commodities that can exogenously arrive at node n .

A NUM framework that is similar to the framework in [8, Sec. 5.1] is considered. In particular, exogenously arriving data are not directly admitted to the NW layer. Instead, the exogenous data are first placed in the transport-layer storage reservoirs. To avoid complications that may arise, which are extraneous to our problem, we assume that all commodities

³We say that a receiver uses *single-user detection* when it decodes each of its intended signals by treating all other interfering signals as noise. Extensions to more advanced *multiuser detection* techniques will be addressed in Section IV.

⁴The extension to the case of unequal bandwidths W_c and noise power spectral densities N_l is straightforward.

have infinite demand at the transport layer. Nevertheless, the RA algorithms proposed in this paper are still applicable when this assumption is relaxed. At each source node, a set of flow controllers decides the amount of each commodity data admitted every time slot in the NW. Let $x_n^s(t)$ denote the amount of data of commodity s admitted in the NW at node n during time slot t . At the NW layer, each node maintains a set of S internal queues for storing the current backlog (or unfinished work) of each commodity. Let $q_n^s(t)$ denote the current backlog of commodity s data stored at node n . We formally let $q_{d_s}^s(t) = 0$, i.e., it is assumed that data that are successfully delivered to their destination exit the NW layer. Associated with each node-commodity pair $(n, s)_{s \in \mathcal{S}_n}$, we define a concave nondecreasing utility function $u_n^s(y)$, which represents the “reward” that is received by sending the data of commodity s from node n to node d_s at a long-term average rate of y [in bits per slot].

The NUM problem under stability constraints can be formulated as [8, Sec. 5]

$$\begin{aligned} & \text{maximize} && \sum_{n \in \mathcal{N}} \sum_{s \in \mathcal{S}_n} u_n^s(y_n^s) \\ & \text{subject to} && \{y_n^s | n \in \mathcal{N}, s \in \mathcal{S}_n\} \in \Lambda, \end{aligned} \quad (2)$$

where the optimization variables are y_n^s , and Λ represents the NW-layer capacity region.⁵

A dynamic cross-layer control algorithm that achieves a utility and is arbitrarily close to the optimal value of (2) has been introduced in [8, Sec. 5]. In particular, the algorithm performance can be characterized as follows:

$$\sum_{n \in \mathcal{N}} \sum_{s \in \mathcal{S}_n} u_n^s(y_n^{*s}) - \liminf_{T \rightarrow \infty} \sum_{n \in \mathcal{N}} \sum_{s \in \mathcal{S}_n} u_n^s \left(\frac{1}{T} \sum_{t=1:T} \mathbb{E}\{x_n^s(t)\} \right) \leq \frac{B}{V}, \quad (3)$$

where $\{y_n^{*s}\}_{n \in \mathcal{N}, s \in \mathcal{S}_n}$ is the optimal solution of (2), $B > 0$ is a well-defined constant, and $V > 0$ is an algorithm parameter that can be used to control the tightness of the achieved utility to the optimal value [8, Sec. 5.2.1]. The details are extraneous to the central objective of this paper. Particularized to our NW model, in every time slot t , the algorithm performs the following steps.

Algorithm 1: Dynamic cross-layer control algorithm [8, Sec. 5.2]

1) *Flow control.* Each node $n \in \mathcal{N}$ solves the following problem:

$$\begin{aligned} & \text{maximize} && \sum_{s \in \mathcal{S}_n} V u_n^s(x_n^s) - x_n^s q_n^s(t) \\ & \text{subject to} && \sum_{s \in \mathcal{S}_n} x_n^s \leq R_n^{\max}, \quad x_n^s \geq 0, \end{aligned} \quad (4)$$

⁵The network-layer capacity region Λ is the closure of the set of all admissible arrival rate vectors that can stably be supported by the network, considering all possible strategies for choosing the control variables to affect routing, scheduling, and RA (including approaches with perfect knowledge of future events) [8, p. 28].

where the variables are $\{x_n^s\}_{s \in \mathcal{S}_n}$. Set $\{x_n^s(t) = x_n^s\}_{s \in \mathcal{S}_n}$. The parameter $V > 0$ is a chosen parameter that affects the algorithm performance [see (3)], and $R_n^{\max} > 0$ is used to control the burstiness of data delivered to the NW layer.

2) *Routing and in-node scheduling.* For each link l , let

$$\begin{aligned} \beta_l(t) &= \max_s \left\{ q_{tran(l)}^s(t) - q_{rec(l)}^s(t), 0 \right\} \\ c_l^*(t) &= \arg \max_s \left\{ q_{tran(l)}^s(t) - q_{rec(l)}^s(t), 0 \right\}. \end{aligned} \quad (5)$$

If $\beta_l(t) > 0$, the commodity that maximizes the differential backlog, i.e., $c_l^*(t)$, is selected for potential routing over link l . This approach is the well-known rule of next-hop transmission under the backpressure algorithm [12].

3) *RA.* The power allocation $\mathbf{P}(t)$ is given by \mathbf{P} , whose entries p_{lc} solve the following problem:

$$\begin{aligned} & \text{maximize} && \sum_{l \in \mathcal{L}} \beta_l(t) \sum_{c \in \mathcal{C}} \log \left(1 + \frac{g_{lc}(t) p_{lc}}{\sigma^2 + \sum_{j \neq l} g_{jlc}(t) p_{jc}} \right) \\ & \text{subject to} && \sum_{c \in \mathcal{C}} \sum_{l \in \mathcal{O}(n)} p_{lc} \leq p_n^{\max}, \quad n \in \mathcal{N} \\ & && p_{lc} \geq 0, l \in \mathcal{L}, c \in \mathcal{C}. \end{aligned} \quad (6)$$

Once the optimal power allocation $\mathbf{P}(t)$ has been determined, compute the rate allocation $r_l(t)$ for all $l \in \mathcal{L}$ by using (1). The resulting rate $r_l(t)$ is offered to the data of commodity $c_l^*(t)$.

In the first step, each node n determines the amount of data of commodity s (i.e., $x_n^s(t)$ for all $s \in \mathcal{S}_n$) that are admitted in the NW based on the current backlogs (i.e., $q_n^s(t)$ for all $s \in \mathcal{S}_n$). In the second step, each node n computes β_l and the corresponding commodity $c_l^*(t)$ for all $l \in \mathcal{O}(n)$. The commodity $c_l^*(t)$ is selected for potential routing over link l during time slot t . Recall that *in-node scheduling* refers to selecting the appropriate commodity, and it should not be confused with the links-scheduling mechanism, which is handled by the RA subproblem, i.e., step 3. The third step is the most difficult part of *Algorithm 1*, which computes the power allocation $\mathbf{P}(t)$ in each link l . Of course, $\mathbf{P}(t)$ implicitly determines the links/channels that should be activated in every time slot t . The power allocation $\mathbf{P}(t)$ is used to determine $r_l(t)$ [see (1)], and the resulting link rate $r_l(t)$ is offered to the data of commodity $c_l^*(t)$. Because our main contribution resides in the RA subproblem (6), extensive explanations of *Algorithm 1* are avoided. However, we refer the reader to [8, Sec. 5] for more details.

III. RESOURCE ALLOCATION SUBPROBLEM

In this section, we focus on the RA subproblem (6). By using standard reformulation techniques, we first show that the RA subproblem is equivalent to a CGP [22]. Then, we obtain a successive approximation algorithm for RA in *bipartite* NWs. Next, we explain the challenges of the RA subproblem

in nonbipartite NWs (e.g., multihop NWs) due to the *self-interference problem*.⁶ Finally, we propose a solution method based on *homotopy methods* [21] together with CGP, which circumvents the aforementioned difficulties.

A. CGP Formalization of the RA Subproblem

Let us denote the objective function of (6) by $f_0(\mathbf{P})$. It can be expressed as

$$f_0(\mathbf{P}) = \sum_{l \in \mathcal{L}} \sum_{c \in \mathcal{C}} \log \left(1 + \frac{g_{lc} p_{lc}}{\sigma^2 + \sum_{j \neq l} g_{jlc} p_{jc}} \right)^{\beta_l} \quad (7)$$

$$= -\log \prod_{l \in \mathcal{L}} \prod_{c \in \mathcal{C}} (1 + \gamma_{lc})^{-\beta_l}, \quad (8)$$

where the time index t was dropped for notational simplicity, and γ_{lc} represents the SINR of link l in channel c , i.e.,

$$\gamma_{lc} = \frac{g_{lc} p_{lc}}{\sigma^2 + \sum_{j \neq l} g_{jlc} p_{jc}}, \quad l \in \mathcal{L}, c \in \mathcal{C}. \quad (9)$$

Because $\log(\cdot)$ is an increasing function, (6) can equivalently be reformulated as

$$\begin{aligned} & \text{minimize} && \prod_{c \in \mathcal{C}} \prod_{l \in \mathcal{L}} (1 + \gamma_{lc})^{-\beta_l} \\ & \text{subject to,} && \gamma_{lc} = \frac{g_{lc} p_{lc}}{\sigma^2 + \sum_{j \neq l} g_{jlc} p_{jc}}, \quad l \in \mathcal{L}, c \in \mathcal{C} \\ & && \sum_{c \in \mathcal{C}} \sum_{l \in \mathcal{O}(n)} p_{lc} \leq p_n^{\max}, \quad n \in \mathcal{N} \\ & && p_{lc} \geq 0, \quad l \in \mathcal{L}, c \in \mathcal{C}, \end{aligned} \quad (10)$$

where the variables are $\{p_{lc}, \gamma_{lc}\}_{l \in \mathcal{L}, c \in \mathcal{C}}$. Now, we consider the related problem, i.e.,

$$\begin{aligned} & \text{minimize} && \prod_{c \in \mathcal{C}} \prod_{l \in \mathcal{L}} (1 + \gamma_{lc})^{-\beta_l} \\ & \text{subject to} && \gamma_{lc} \leq \frac{g_{lc} p_{lc}}{\sigma^2 + \sum_{j \neq l} g_{jlc} p_{jc}}, \quad l \in \mathcal{L}, c \in \mathcal{C} \\ & && \sum_{c \in \mathcal{C}} \sum_{l \in \mathcal{O}(n)} p_{lc} \leq p_n^{\max}, \quad n \in \mathcal{N} \\ & && p_{lc} \geq 0, \quad l \in \mathcal{L}, c \in \mathcal{C} \end{aligned} \quad (11)$$

with the same variables $\{p_{lc}, \gamma_{lc}\}_{l \in \mathcal{L}, c \in \mathcal{C}}$. Note that the equality constraints of (10) have been replaced with inequality constraints. We refer to these inequality constraints as SINR constraints for simplicity. Because the objective function of (11) increases in each γ_{lc} , we can guarantee that, at any optimal solution of (11), the SINR constraints must be active. Therefore, we solve (11) instead of (10).

Finally, by introducing the auxiliary variables $v_{lc} \leq 1 + \gamma_{lc}$ and rearranging the terms, the RA subproblem (6) can be further

reformulated as

$$\begin{aligned} & \text{minimize} && \prod_{c \in \mathcal{C}} \prod_{l \in \mathcal{L}} v_{lc}^{-\beta_l} \\ & \text{subject to} && v_{lc} \leq 1 + \gamma_{lc}, \quad l \in \mathcal{L}, c \in \mathcal{C} \\ & && \sigma^2 g_{lc}^{-1} p_{lc}^{-1} \gamma_{lc} + \sum_{j \neq l} g_{llc}^{-1} g_{jlc} p_{jc} p_{lc}^{-1} \gamma_{lc} \\ & && \leq 1, \quad l \in \mathcal{L}, c \in \mathcal{C} \\ & && \sum_{c \in \mathcal{C}} \sum_{l \in \mathcal{O}(n)} (p_n^{\max})^{-1} p_{lc} \leq 1, \quad n \in \mathcal{N} \\ & && p_{lc} \geq 0, \quad l \in \mathcal{L}, c \in \mathcal{C}, \end{aligned} \quad (12)$$

which can be identified as a CGP [22].

B. Successive Approximation Algorithm for RA in Bipartite NWs ($\mathcal{A} = \emptyset$)

By inspecting (12), we notice the following three cases: 1) The objective is a monomial⁷ function; 2) the right-hand side (RHS) terms of the first inequality constraints (i.e., $1 + \gamma_{lc}$) are posynomial functions; and 3) the left-hand side terms of all the inequality constraints are either monomial or posynomial functions. Note that, if the RHS terms of the first inequality constraints were monomial (instead of posynomial) functions, (12) will become a geometric program (GP) in standard form. GPs can be reformulated as convex problems, and they can very efficiently be solved, even for large-scale problems [36, Sec. 2.5]. These observations suggest that, by starting from an initial point, we can search for a close local optimum by solving a sequence of GPs that locally approximate the original problem (12). At each step, the GP is obtained by replacing the posynomial functions in the RHS of the first inequality constraints with their best local monomial approximations near the solution obtained at the previous step. The solution methods that are achieved by monomial approximations [22], [36] can be considered to be a subset of a broader class of mathematical optimization problems, which is known in the mathematical literature as *inner approximation algorithms for nonconvex problems* [44]. The monomial approximation for the RHS terms of the first inequality constraints in (12) is described in the following lemma.

Lemma 1: For any $\gamma > 0$, let $m(\gamma) = k\gamma^a$ be a monomial function that is used to approximate $s(\gamma) = 1 + \gamma$ near an arbitrary point $\hat{\gamma} > 0$. Then, the following two conditions hold.

- 1) The parameters a and k of the best monomial local approximation are given by

$$a = \hat{\gamma}(1 + \hat{\gamma})^{-1}, \quad k = \hat{\gamma}^{-a}(1 + \hat{\gamma}). \quad (13)$$

- 2) $s(\gamma) \geq m(\gamma)$ for all $\gamma > 0$.

Proof: To show the first part, we note that the monomial function m is the best local approximation of s near the point $\hat{\gamma}$ if

$$m(\hat{\gamma}) = s(\hat{\gamma}), \quad m'(\hat{\gamma}) = s'(\hat{\gamma}). \quad (14)$$

⁶When a node simultaneously transmits and receives in the same channel, its incoming links are affected by very large self interference levels.

⁷See [36, Sec. 2.1] for the definition of monomial and posynomial functions.

By replacing the expressions of m and s in (14), we obtain the following system of equations:

$$\begin{cases} k\hat{\gamma}^a = 1 + \hat{\gamma} \\ ka\hat{\gamma}^{a-1} = 1 \end{cases} \quad (15)$$

the solution of which is given by (13).

The second part follows from (14) and by noting that $s(\gamma)$ is affine and $m(\gamma)$ is concave⁸ on \mathbb{R}_+ . ■

Now, we turn to the GP obtained by using the local approximation given by Lemma 1. The posynomial functions $1 + \gamma_{lc}$ of the first inequality constraints of (12) are approximated near the point $\hat{\gamma}_{lc}$. Consequently, the approximate inequality constraints become

$$v_{lc} \leq k_{lc}\gamma_{lc}^{a_{lc}}, \quad l \in \mathcal{L}, c \in \mathcal{C}, \quad (16)$$

where a_{lc} and k_{lc} have the forms given in (13). Because the objective function of (12) is a decreasing function of v_{lc} , $l \in \mathcal{L}$, $c \in \mathcal{C}$, it can easily be verified that all of these modified inequality constraints will be active at the solution of the GP. Therefore, we can eliminate the auxiliary variables v_{lc} and rewrite the objective function of (12) as

$$\prod_{l \in \mathcal{L}} \prod_{c \in \mathcal{C}} v_{lc}^{-\beta_l} = \prod_{l \in \mathcal{L}} \prod_{c \in \mathcal{C}} k_{lc}^{-\beta_l} \gamma_{lc}^{-\beta_l a_{lc}} = K \prod_{l \in \mathcal{L}} \prod_{c \in \mathcal{C}} \gamma_{lc}^{-\beta_l \frac{\hat{\gamma}_{lc}}{1 + \hat{\gamma}_{lc}}}, \quad (17)$$

where K is a multiplicative constant that does not affect the problem solution.

In the following sections, we base our development on computationally efficient algorithms to obtain a suboptimal solution for (11). For notational convenience, it is useful to define the overall SINR matrices $\gamma, \hat{\gamma} \in \mathbb{R}_+^{L \times C}$ as $[\gamma]_{l,c} = \gamma_{lc}$ and $[\hat{\gamma}]_{l,c} = \hat{\gamma}_{lc}$, respectively.

A very brief outline of the proposed successive approximation algorithm is given as follows. It solves an approximated version of (12) in every iteration, and the algorithm consists of repeating this step until convergence.

Algorithm 2: Successive approximation algorithm for RA

- 1) *Initialization.* Given tolerance $\epsilon > 0$, a feasible power allocation \mathbf{P}_0 . Set $i = 1$. The initial SINR guess $\hat{\gamma}^{(i)}$ is given by (9).
- 2) Solve the GP

$$\begin{aligned} &\text{minimize} && K^{(i)} \prod_{l \in \mathcal{L}} \prod_{c \in \mathcal{C}} \gamma_{lc}^{-\beta_l \frac{\hat{\gamma}_{lc}^{(i)}}{1 + \hat{\gamma}_{lc}^{(i)}}} \\ &\text{subject to} && \alpha^{-1} \hat{\gamma}_{lc}^{(i)} \leq \gamma_{lc} \leq \alpha \hat{\gamma}_{lc}^{(i)}, \quad l \in \mathcal{L}, c \in \mathcal{C} \\ &&& \sigma^2 g_{llc}^{-1} p_{lc}^{-1} \gamma_{lc} + \sum_{j \neq l} g_{llc}^{-1} g_{jlc} p_{jc} p_{lc}^{-1} \gamma_{lc} \\ &&& \leq 1, \quad l \in \mathcal{L}, c \in \mathcal{C} \\ &&& \sum_{c \in \mathcal{C}} \sum_{l \in \mathcal{O}(n)} (p_n^{\max})^{-1} p_{lc} \leq 1, \quad n \in \mathcal{N} \quad (18) \end{aligned}$$

⁸The concavity of $m(\gamma)$ follows from the fact that $k > 0$ and $0 < a < 1$ [45, Sec. 3.1.5].

with the positive variables $\{p_{lc}, \gamma_{lc}\}_{l \in \mathcal{L}, c \in \mathcal{C}}$. Denote the solution by $\{p_{lc}^*, \gamma_{lc}^*\}_{l \in \mathcal{L}, c \in \mathcal{C}}$.

- 3) *Stopping criterion.* If $\max_{(l,c) \in \mathcal{L} \times \mathcal{C}} |\gamma_{lc}^* - \hat{\gamma}_{lc}^{(i)}| \leq \epsilon$, stop; otherwise, go to step 4.
- 4) Set $i = i + 1$, $\{\hat{\gamma}_{lc}^{(i)} = \gamma_{lc}^*\}_{l \in \mathcal{L}, c \in \mathcal{C}}$, and go to step 2.

The first step initializes the algorithm, and an initial feasible SINR guess $\hat{\gamma}^{(i)}$ is computed. For bipartite NWs, there is no *self-interference problem*, and a simple uniform power allocation can be used.

The second step solves an equivalent GP approximation of (12) around the current guess $\hat{\gamma}^{(i)}$ [see (18)]. Note that the auxiliary variables $\{v_{lc}\}_{c \in \mathcal{C}, l \in \mathcal{L}}$ of (12) are eliminated and the objective function of (12) is replaced by using the monomial approximation at $\hat{\gamma}^{(i)}$, as given in (17).⁹ These monomial approximations are sufficiently accurate only in the closer vicinity of the current guess $\hat{\gamma}^{(i)}$. Therefore, the first set of inequality constraints are added to confine the domain of variables γ to a region around the current guess $\hat{\gamma}^{(i)}$ [46]. The first set of inequality constraints of (18) are sometimes called trust region constraints [36], [46], which are not originally introduced in [22]. Therefore, *Algorithm 2* is a slightly modified version of the solution method proposed in [22]. The parameter $\alpha > 1$ controls the desired approximation accuracy. However, it also influences the convergence speed of *Algorithm 2*. At every step, each entry of the current SINR guess $\hat{\gamma}^{(i)}$ can be increased or decreased at most by a factor α . Thus, a value of α that is close to 1 provides good accuracy for the monomial approximations, at the cost of slower convergence speed, whereas a value much that is larger than 1 improves the convergence speed, at the cost of reduced accuracy. In most practical cases, a fixed value $\alpha = 1.1$ offers a good speed/accuracy tradeoff [36].

The third step checks whether the SINRs $\{\gamma_{lc}^*\}_{l \in \mathcal{L}, c \in \mathcal{C}}$ that are obtained from the solution of (18) have significantly been changed compared to the entries of the current guess $\hat{\gamma}^{(i)}$. If there are no substantial changes, then the algorithm terminates, and the link rate $r_l(t) = \sum_{c=1}^C W_c \log(1 + \gamma_{lc}^*)$ is offered to the data of commodity $c_l^*(t)$ [given by (5)]. Otherwise, the solution $\{\gamma_{lc}^*\}_{l \in \mathcal{L}, c \in \mathcal{C}}$ is taken as the current guess, and the algorithm repeats steps 2–4 until convergence.

Note that the auxiliary variables $\{v_{lc}\}_{c \in \mathcal{C}, l \in \mathcal{L}}$ were only used to reformulate (11) as a CGP [22], i.e., (12), but they do not appear in *Algorithm 2*. In fact, an identical algorithm results if, at each step, the objective function of (11) is locally approximated by a monomial function. This alternative derivation, which is known in the optimization literature as SP [36], is presented in Appendix A.

The convergence of the algorithm to a Kuhn–Tucker solution of the original nonconvex problem (12) is guaranteed [44, Th. 1], because *Algorithm 2* falls into the broader class of mathematical optimization problems, i.e., *inner approximation algorithms for nonconvex problems* [44].

One interesting and important remark is that the objective function of the approximated problem (18) in each iteration i

⁹Recall that $K^{(i)}$ is a multiplicative constant that does not influence the solution of (18).

yields an upper bound on the objective function of the original problem (11), i.e.,

$$K^{(i)} \prod_{l \in \mathcal{L}} \prod_{c \in \mathcal{C}} \gamma_{lc}^{-\beta_l \frac{\hat{\gamma}_{lc}^{(i)}}{1 + \hat{\gamma}_{lc}^{(i)}}} \geq \prod_{l \in \mathcal{L}} \prod_{c \in \mathcal{C}} (1 + \gamma_{lc})^{-\beta_l} \quad (19)$$

for $\{\gamma_{lc} > 0\}_{l \in \mathcal{L}, c \in \mathcal{C}}$, with equality when $\gamma = \hat{\gamma}^{(i)}$. This case directly follows from the second statement of Lemma 1. By using (19), we can immediately show that *Algorithm 2* is monotonically decreasing. The monotonicity of *Algorithm 2* is established by the following theorem.

Theorem 1: Let i and $i + 1$ be any consecutive iteration of *Algorithm 2*. Let $\hat{\gamma}^{(i)}$ and $\hat{\gamma}^{(i+1)}$ be the SINR guesses at the beginning of each iteration, respectively. Then

$$\prod_{l \in \mathcal{L}} \prod_{c \in \mathcal{C}} (1 + \hat{\gamma}_{lc}^{(i)})^{-\beta_l} \geq \prod_{l \in \mathcal{L}} \prod_{c \in \mathcal{C}} (1 + \hat{\gamma}_{lc}^{(i+1)})^{-\beta_l}. \quad (20)$$

Proof: To show this proof, we write the following relations:

$$\prod_{l \in \mathcal{L}} \prod_{c \in \mathcal{C}} (1 + \hat{\gamma}_{lc}^{(i)})^{-\beta_l} = K^{(i)} \prod_{l \in \mathcal{L}} \prod_{c \in \mathcal{C}} (\hat{\gamma}_{lc}^{(i)})^{-\beta_l \frac{\hat{\gamma}_{lc}^{(i)}}{1 + \hat{\gamma}_{lc}^{(i)}}} \quad (21)$$

$$\geq K^{(i)} \prod_{l \in \mathcal{L}} \prod_{c \in \mathcal{C}} (\hat{\gamma}_{lc}^{(i+1)})^{-\beta_l \frac{\hat{\gamma}_{lc}^{(i)}}{1 + \hat{\gamma}_{lc}^{(i)}}} \quad (22)$$

$$\geq \prod_{l \in \mathcal{L}} \prod_{c \in \mathcal{C}} (1 + \hat{\gamma}_{lc}^{(i+1)})^{-\beta_l}, \quad (23)$$

where (21) follows from (19) and (22) because $\hat{\gamma}^{(i+1)}$ is the solution of (18), and (23) again follows from (19). ■

Therefore, we immediately see that *Algorithm 2* always yields a solution that is at least as good as the solution in the previous iteration. This is important in the context of practical implementations, because in practice, we can always stop the algorithm within a few iterations before it terminates.

C. Self-Interference Problem

Let us now consider the nonbipartite NWs. According to Section II-A, for such NWs, we have $\mathcal{A} \neq \emptyset$. In other words, the set of nodes cannot be divided into two distinct subsets \mathcal{T} and \mathcal{R} , i.e., $\mathcal{T} \cap \mathcal{R} \neq \emptyset$ (e.g., multihop wireless NWs). For example, see Figs. 1 and 2. For such NW topologies, there is a *self-interference problem*, and consequently, the RA problem must also cope with the self-interference problem. The difficulty comes from the fact that the self-interference gains $\{g_{ijc}\}_{(i,j) \in \mathcal{A}}$ are typically few orders of magnitude larger than the power gains between distinct NW nodes $\{g_{jjc}\}_{j \in \mathcal{L}}$. Therefore, there is a huge imbalance between some entries of $\{g_{ijc}\}_{i,j \in \mathcal{L}}$. Roughly speaking, this condition can destroy the smoothness of the functions that are associated with the RA problem, e.g., the objective function of (6), and can ruin the reliability and the efficiency of *Algorithm 2*, which at least suboptimally solves it. In other words, there can be several highly suboptimal Kuhn–Tucker solutions for (12), at which *Algorithm 2* can terminate by returning a very bad suboptimal

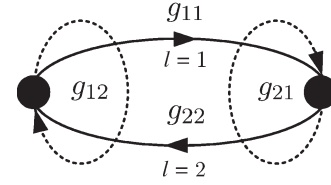


Fig. 2. Two-node NW (the channel c and time t indices are omitted for clarity), where $\mathcal{A} = \{(1, 2), (2, 1)\}$, $g_{12} = 1$, $g_{21} = 1$, $g_{11} = |h_{11}|^2$, and $g_{22} = |h_{22}|^2$.

solution. Moreover, the SINR values at the incoming links of a node that simultaneously transmits in the same channel are very small, and the convergence of *Algorithm 2* can be very slow if it starts with an initial SINR guess $\hat{\gamma}$ that contains entries with nearly zero values. Therefore, the direct application of *Algorithm 2* almost always performs very poorly, and further improvements are necessary.

One standard way of dealing with the self-interference problem consists of adding a supplementary combinatorial constraint in the RA subproblem that does not allow any node in the NW to simultaneously transmit and receive in the same channel [41]–[43]. We will refer to a power allocation that satisfies this constraint as *admissible*. Note that this approach will require solving a power optimization problem (by using *Algorithm 2*) for each possible subset of links that can simultaneously be activated. This approach results in a combinatorial nature for the RA subproblem in the case of nonbipartite NWs [47]–[53]. Of course, because the complexity of this approach exponentially grows with the number of links and the number of channels, this solution method quickly becomes impractical.

D. Successive Approximation Algorithm for RA in Nonbipartite NWs ($\mathcal{A} \neq \emptyset$): A Homotopy Method

To avoid the difficulties pointed out in Section III-C, we propose an algorithm that is inspired by *homotopy methods* [21] that can be traced back to the late 1980s; see [54] and the references therein. In fact, the well-known interior-point methods [55] [45, Sec. 11] for convex optimization problems also fall into this general class of homotopy methods.

The underlying idea is to first introduce a parameterized problem that approximates the original problem (11). In particular, we construct the parameterized problem from the original problem (11) by setting $g_{ijc} = g$ for all $(i, j) \in \mathcal{A}$, where $g > 0$ is referred to as the homotopy parameter. Note that the quality of the approximation improves as g grows. Of course, when g is small (e.g., g and g_{jjc} are roughly in the same order), *Algorithm 2* can reliably be used to find a suboptimal solution for the parameterized problem. On the other hand, when g is large (e.g., $g = 1$), the parameterized problem is exactly the same as the original problem (11), and therefore, *Algorithm 2* cannot reliably perform, i.e., it becomes very slow, and its result become strongly dependent on the initialization. Thus, to circumvent this difficulty, a sequence of parameterized problems are solved, starting from a very small g and increasing the parameter g (thus, the accuracy of the approximation) at each step until $g = 1$. Moreover, in each step, when solving the parameterized problem for the current value of g , the initial

guess for *Algorithm 2* is obtained by using the solution (power) of the parameterized problem for the previous value of g .

The proposed algorithm, which based on homotopy methods, can be summarized as follows.

Algorithm 3: Successive approximation algorithm for RA in the presence of self interferers

- 1) *Initialization*. Given an initial homotopy parameter $g_0 < 1$, $\rho > 1$, a feasible power allocation \mathbf{P}_0 . Let $g = g_0$, $\mathbf{P} = \mathbf{P}_0$.
 - 2) Set $g_{ijc} = g$ for all $(i, j) \in \mathcal{A}$. Find the SINR guess $\hat{\gamma}$ by using (9).
 - 3) *Solving the parameterized problem*. Let $\hat{\gamma}^{(1)} = \hat{\gamma}$ and perform steps 2–4 of *Algorithm 2* until convergence to obtain the power and SINR values $\{p_{lc}^*, \gamma_{lc}^*\}_{l \in \mathcal{L}, c \in \mathcal{C}}$. Let $\{p_{lc} = p_{lc}^*\}_{l \in \mathcal{L}, c \in \mathcal{C}}$.
 - 4) If $\exists (i, j) \in \mathcal{A}$ and $c \in \mathcal{C}$ such that $p_{ic}p_{jc} > 0$ (i.e., \mathbf{P} is not admissible), then set $g = \min\{\rho g, 1\}$ and go to step 5. Otherwise, i.e., \mathbf{P} is admissible, stop.
 - 5) If $g < 1$, go to step 2; otherwise, stop.
-

The first step initializes the algorithm, and the homotopy parameter g is initialized by g_0 , where g_0 is chosen in the same range of values as the power gains between distinct nodes. In particular, in our simulations, we select $g_0 = \max_{j \in \mathcal{L}} \{g_{jjc}\}$. Step 2 updates the problem data for the parameterized problem and a feasible SINR guess is computed. The third step finds a suboptimal solution for the parameterized problem. The algorithm terminates in step 4 if \mathbf{P} is admissible (thus, none of the nodes in the NW simultaneously transmits and receives in the same channel). On the other hand, if \mathbf{P} is not admissible, then the homotopy parameter g is increased. If g reaches its extreme allowed value (i.e., the actual self-interference gain value of 1), the algorithm terminates. Otherwise, i.e., $g < 1$, it returns to step 2 and continues. Terminating *Algorithm 3* if the solution is *admissible* is intuitively obvious for the following reason. The data that are associated with the parameterized problem that is solved in step 3 of *Algorithm 3* become independent of the homotopy parameter g , and therefore, further increase in g after having an *admissible* solution has no effect on the results. Our computational experience suggests that *Algorithm 3* yields an *admissible* solution way before g reaches a value of 1 (e.g., by selecting $\rho = 2$ in all our simulations, an admissible power allocation is achieved in about one to four iterations).

Because *Algorithm 3* runs a finite number of instances of *Algorithm 2*, its computational complexity *does not increase* more than polynomially with the problem size. Clearly, *Algorithm 3* can converge to a Kuhn–Tucker solution of the last parameterized problem (one just before the termination of *Algorithm 3*).

As a specific example of illustrating the self interference, i.e., $\mathcal{A} \neq \emptyset$, consider the simple NW shown in Fig. 2. Here, $N = 2$, $L = 2$, and $C = 1$. Note that $\mathcal{A} = \{(1, 2), (2, 1)\}$, and let $\beta_1, \beta_2 \neq 0$. Suppose that $g_{12} \gg g_{22}$ and $g_{21} \gg g_{11}$, which is often the case due to path losses. Because the gains $g_{12} = 1$ and $g_{21} = 1$ are very large compared with g_{22} and g_{11} , for any

nonzero power allocation $p_1, p_2 = p_0$, the initial SINR guess $\hat{\gamma}_1, \hat{\gamma}_2$ will have nearly zero values. This case results in difficulties of directly using *Algorithm 2*. In *Algorithm 3*, this problem is circumvented by initializing the gains g_{12} and g_{21} by a parameter g_0 (e.g., $g_0 = \max\{g_{11}, g_{22}\}$) and repeatedly executing *Algorithm 2*, incrementally increasing the parameter g until it reaches 1, which is the true value of g_{12} and g_{21} .

With regard to the complexity of the proposed algorithm, we make the following remarks. The computational complexity of a GP depends on the number of variables and constraints, as well as on the sparsity pattern of the problem [36]. Unfortunately, it is difficult to precisely quantify the sparsity pattern, and therefore, a general complexity analysis is not available. To give a rough idea, let us consider a fully connected NW with $N = 9$ nodes and $C = 8$ channels. The number of variables in (18) is $2LC = 1152$, the number of constraints is $3LC + N = 1737$, and it was solved in about 12 s on a desktop computer. The number of iterations depends on the starting point p_n^{\max} and channel gains g_{ijc} , but typically, *Algorithm 2* required around 100 iterations to converge.

Nevertheless, with some slight modifications, it is possible to dramatically decrease the average complexity per iteration, which is very important in the context of practical implementations. Two simple modifications are as given follows.

- 1) Use large values for the parameter α in *Algorithm 2*. As discussed in Section III-B, a large α can improve the convergence speed of *Algorithm 2*, at the cost of reduced accuracy of the monomial approximation.
- 2) Eliminate (relatively) insignificant variables. We can eliminate the power variables p_{lc} and the associated SINR variables γ_{lc} from (18) when they have relatively very small contributions to the overall objective value of (18).

In particular, the exponent term $\beta_l(\hat{\gamma}_{lc}^{(i)}/1 + \hat{\gamma}_{lc}^{(i)})$ in the objective of (18) is evaluated for all $l \in \mathcal{L}$, $c \in \mathcal{C}$. If $\beta_l(\hat{\gamma}_{lc}^{(i)}/1 + \hat{\gamma}_{lc}^{(i)}) \ll \max_{\bar{l} \in \mathcal{L}, \bar{c} \in \mathcal{C}} (\beta_{\bar{l}}(\hat{\gamma}_{\bar{l}\bar{c}}^{(i)}/1 + \hat{\gamma}_{\bar{l}\bar{c}}^{(i)}))$ then p_{lc} s and the associated γ_{lc} s are eliminated in successive GPs.

IV. EXTENSION TO THE MULTIUSER DETECTOR CASE

The receiver structure has basically been assumed to be equivalent to a bank of match filters, each of which attempts to decode one of the signals of interest at each node while treating the other signals as noise. This is a suboptimal detector structure that is commonly assumed. In this section, we investigate the possible gains that are achievable by using more advanced receiver structures. For clarity, we first discuss the single-channel case. The extension to the multichannel case is presented in Appendix B. We assume that, at every node $n \in \mathcal{N}$, the transmitter performs superposition coding over its outgoing links $\mathcal{O}(n)$ and the receiver decodes the signals of incoming links $\mathcal{I}(n)$ by using a MU receiver based on the successive interference cancellation (SIC) strategy. We may, of course, assume other detector structures, including the optimum approach that implements maximum likelihood. The largest set of achievable rates is obtained when the SIC receiver at every node $n \in \mathcal{N}$ is allowed to decode and cancel out the signals of all its incoming links $\mathcal{I}(n)$ and any subset of the remaining

links in its complement set $\mathcal{L} \setminus \mathcal{I}(n)$. Let $\mathcal{D}(n)$ denote the set of links that are decoded at the node n , i.e., $\mathcal{D}(n) = \mathcal{I}(n) \cup \mathcal{U}(n)$ for some $\mathcal{U}(n) \subseteq \mathcal{L} \setminus \mathcal{I}(n)$. Furthermore, let $\mathcal{R}^{\text{SIC}}(\mathcal{D}(1), \dots, \mathcal{D}(N), p_1^{\max}, \dots, p_N^{\max})$ denote the achievable rate region for given $\mathcal{D}(1), \dots, \mathcal{D}(N)$ and maximum node transmission power $p_1^{\max}, \dots, p_N^{\max}$. We denote by $\mathcal{R}^{\text{SIC}}(p_1^{\max}, \dots, p_N^{\max})$ the achievable rate region that is obtained as a union of all $\mathcal{R}^{\text{SIC}}(\mathcal{D}(1), \dots, \mathcal{D}(N), p_1^{\max}, \dots, p_N^{\max})$ over all possible $2^{\sum_{n \in \mathcal{N}} (L - |\mathcal{I}(n)|)}$ combinations of sets $\mathcal{D}(1), \dots, \mathcal{D}(N)$, i.e.,

$$\begin{aligned} & \mathcal{R}^{\text{SIC}}(p_1^{\max}, \dots, p_N^{\max}) \\ &= \bigcup_{\mathcal{D}(1), \dots, \mathcal{D}(N) | \forall n \in \mathcal{N} \exists \mathcal{U}(n) \subseteq \mathcal{L} \setminus \mathcal{I}(n) \text{ s.t. } \mathcal{D}(n) = \mathcal{I}(n) \cup \mathcal{U}(n)} \mathcal{R}^{\text{SIC}}(\mathcal{D}(1), \dots, \mathcal{D}(N), p_1^{\max}, \dots, p_N^{\max}). \end{aligned} \quad (24)$$

The receiver of each node $n \in \mathcal{N}$ is allowed to perform SIC in its own order. Let $\pi_n = (\pi_n(1), \dots, \pi_n(|\mathcal{D}(n)|))$ be an arbitrary permutation of the links in $\mathcal{D}(n)$, which describes the decoding and cancelation order at node n . In particular, the signal of link $\pi_n(l)$ is decoded after all codewords of links $\pi_n(j)$, $j < l$, have been decoded and their contribution to the signal received at node n has been canceled. Thus, only the signals of the links $\pi_n(j)$, $j > l$, act as interference. The rate region $\mathcal{R}^{\text{SIC}}(\mathcal{D}(1), \dots, \mathcal{D}(N), p_1^{\max}, \dots, p_N^{\max})$ is obtained by considering all possible combinations of decoding orders for all nodes, i.e., all possible $\prod_{n \in \mathcal{N}} (|\mathcal{D}(n)|!)$ combinations $\pi \triangleq \pi_1 \times \pi_2 \times \dots \times \pi_N$. Thus, $\mathcal{R}^{\text{SIC}}(\mathcal{D}(1), \dots, \mathcal{D}(N), p_1^{\max}, \dots, p_N^{\max})$ can be expressed as in (25), shown at the bottom of the page. Here, G_{ln} , $l \in \mathcal{L}$, $n \in \mathcal{N}$ represents the power gain from the transmitter of link l to the receiver at node n , and p_l represents the power that is allocated for the signal of link l . Clearly, the computational complexity experiences a formidable increase. Nevertheless, the RA subproblem at the third step of the dynamic cross-layer control *Algorithm 1* can be written as¹⁰

$$\begin{aligned} & \text{maximize} && \sum_{l \in \mathcal{L}} \beta_l(t) r_l \\ & \text{subject to} && (r_1, \dots, r_L) \in \mathcal{R}^{\text{SIC}}(p_1^{\max}, \dots, p_N^{\max}). \end{aligned} \quad (26)$$

The combinatorial description of $\mathcal{R}^{\text{SIC}}(p_1^{\max}, \dots, p_N^{\max})$ implies that solving (26) requires optimization over all possible combinations of decoding sets $\mathcal{D}(1), \dots, \mathcal{D}(N)$ and decoding

¹⁰Note that $\mathcal{R}^{\text{SIC}}(p_1^{\max}, \dots, p_N^{\max})$ represents the set of *directly achievable* rates. By invoking a time-sharing argument, we can extend the achievable rate region to the convex hull of $\mathcal{R}^{\text{SIC}}(p_1^{\max}, \dots, p_N^{\max})$. However, this approach will not affect the optimal value of (26), because the objective function is linear [3].

orders π . This approach is intractable, even for the offline optimization of moderate-size NWs. Therefore, in the following discussion, we propose two alternatives for finding the solution of a more constrained version of (26) instead of solving (26). The first alternative limits the access protocol so that only one node can transmit in all its outgoing links in each time slot. The second alternative adopts a similar view by assuming that only one node can receive from all its incoming links in each time slot. The main advantage of the aforementioned alternatives is their simplicity. As a result, a cheaply computable lower bound on the optimal value of (26) can be obtained. Moreover, these simple access protocols can be useful in practical applications with more advanced communication systems.

A. Single-Node Transmission Case

By imposing the additional constraint that only one node can transmit during each slot, the RA subproblem (26) is reduced to a problem where the optimal power and rate allocation can be computed through convex programming. In particular, the RA subproblem (26) is reduced to N weighted sum-rate maximization problems for the scalar broadcast channel: one for each possible transmitting node.

For any node $n \in \mathcal{N}$, let $\rho_n = (\rho_n(1), \dots, \rho_n(|\mathcal{O}(n)|))$ be a permutation of the set of outgoing links $\mathcal{O}(n)$ such that

$$g_{\rho_n(1)\rho_n(1)}(t) \leq g_{\rho_n(2)\rho_n(2)}(t) \leq \dots \leq g_{\rho_n(|\mathcal{O}(n)|)\rho_n(|\mathcal{O}(n)|)}(t),$$

where $g_{ij}(t)$ denotes the power gain from the transmitter of link i to the receiver of link j during time slot t . Now, we consider the case where node n is the transmitter. This condition results in a scalar Gaussian broadcast channel with $|\mathcal{O}(n)|$ users. The optimal decoding and cancelation order at every receiver node of links $\rho_n(i)$, $i \in \{1, \dots, |\mathcal{O}(n)|\}$ is specified by ρ_n [56, Sec. 6]. In particular, the receiver of the link $\rho_n(i)$ decodes its own signal after all codewords of links $\rho_n(j)$, $j < i$ have been decoded and their contribution to the received signal has been canceled. Thus, only the signals of the links $\rho_n(j)$, $j > i$, act as interference at the receiver of the link $\rho_n(i)$. Now, we can rewrite (26) by using the capacity region descriptions of the scalar Gaussian broadcast channels [57] as

$$\begin{aligned} & \text{maximize} && \sum_{l \in \mathcal{O}(n)} \beta_l r_l \\ & \text{subject to} && n \in \mathcal{N} \\ & && r_{\rho_n(i)} \leq \log \left(1 + \frac{g_{\rho_n(i)\rho_n(i)} p_{\rho_n(i)}}{\sigma^2 + g_{\rho_n(i)\rho_n(i)} \sum_{j=i+1}^{|\mathcal{O}(n)|} p_{\rho_n(j)}} \right) \\ & && i \in \{1, \dots, |\mathcal{O}(n)|\} \end{aligned}$$

$$\begin{aligned} & \mathcal{R}^{\text{SIC}}(\mathcal{D}(1), \dots, \mathcal{D}(N), p_1^{\max}, \dots, p_N^{\max}) \\ &= \bigcup_{\pi} \left\{ (r_1, \dots, r_L) \left| \begin{array}{l} r_{\pi_n(l)} \leq \log \left(1 + \frac{G_{\pi_n(l)n}(t) p_{\pi_n(l)}}{\sigma^2 + \sum_{j>l} G_{\pi_n(j)n}(t) p_{\pi_n(j)}} \right), \quad \forall (n, l) \text{ s.t. } n \in \mathcal{N}, l \in \{1, \dots, |\mathcal{D}(n)|\} \\ \sum_{l \in \mathcal{O}(n)} p_l \leq p_n^{\max}, \\ p_l \geq 0, \end{array} \right. \right. \\ & && \left. \left. \begin{array}{l} n \in \mathcal{N} \\ l \in \mathcal{L} \end{array} \right\} \end{array} \right\} \quad (25)$$

$$\begin{aligned}
 \sum_{l \in \mathcal{O}(n)} p_l &\leq p_n^{\max} \\
 p_l &\geq 0 \quad l \in \mathcal{O}(n) \\
 p_l &= 0 \quad l \notin \mathcal{O}(n),
 \end{aligned} \tag{27}$$

where the variables are n , p_l , and r_l . Note that the time index t is dropped for notational convenience. The solution of (27) is obtained in two steps. First, we solve N independent subproblems (one subproblem for each possible transmitting node $n \in \mathcal{N}$). Then, we select the solution of the subproblem with the largest objective value. The subproblem can be expressed as

$$\begin{aligned}
 &\text{maximize} \quad \sum_{i=1}^{|\mathcal{O}(n)|} \beta_{\rho_n(i)} r_{\rho_n(i)} \\
 &\text{subject to} \quad r_{\rho_n(i)} = \log \left(1 + \frac{g_{\rho_n(i)\rho_n(i)} p_{\rho_n(i)}}{\sigma^2 + g_{\rho_n(i)\rho_n(i)} \sum_{j=i+1}^{|\mathcal{O}(n)|} p_{\rho_n(j)}} \right) \\
 &\quad \quad \quad i \in \{1, \dots, |\mathcal{O}(n)|\} \\
 &\quad \quad \quad \sum_{l \in \mathcal{O}(n)} p_l \leq p_n^{\max} \\
 &\quad \quad \quad p_l \geq 0, \quad l \in \mathcal{O}(n),
 \end{aligned} \tag{28}$$

where the variables are r_l and p_l , $l \in \mathcal{O}(n)$. Problem (28) represents the weighted sum-rate maximization over the capacity region of a scalar Gaussian broadcast channel [57, Sec. 2] with $|\mathcal{O}(n)|$ users. The *barrier method* [45, Sec. 11.3.1] or the explicit greedy method proposed in [57, Sec. 3.2] can be used to efficiently solve this problem. Here, we use the *barrier method*; see Appendix C for more details. Let $g^{(n)}$, $p_l^{(n)}$, and $r_l^{(n)}$ denote the optimal objective value and the corresponding optimal solution, i.e., power and rate, respectively. Then, the rate/power relation can be expressed as

$$r_{\rho_n(i)}^{(n)} = \log \left(1 + \frac{g_{\rho_n(i)\rho_n(i)} p_{\rho_n(i)}^{(n)}}{\sigma^2 + g_{\rho_n(i)\rho_n(i)} \sum_{j=i+1}^{|\mathcal{O}(n)|} p_{\rho_n(j)}^{(n)}} \right) \quad i \in \{1, \dots, |\mathcal{O}(n)|\} \tag{29}$$

and the optimal solution of (27) is given by

$$\begin{aligned}
 n^* &= \arg \max_{n \in \mathcal{N}} g^{(n)} \\
 p_l^* &= \begin{cases} p_l^{(n^*)} & l \in \mathcal{O}(n^*) \\ 0 & \text{otherwise} \end{cases} \\
 r_l^* &= \begin{cases} r_l^{(n^*)} & l \in \mathcal{O}(n^*) \\ 0 & \text{otherwise.} \end{cases}
 \end{aligned} \tag{30}$$

B. Single-Node Reception Case

Here, we consider the case where only one node can receive during each slot. As a result, the associated RA subproblem (26) is reduced to a simpler form, where the optimal power and rate allocation can very efficiently be computed by considering N weighted sum-rate maximization problems for the Gaussian multiaccess channel: one for each possible receiving node.

We start by considering the capacity region descriptions of the Gaussian multiaccess channel with $|\mathcal{I}(n)|$, $n \in \mathcal{N}$ users [58], [56, Sec. 6]. For any receiving node $n \in \mathcal{N}$, the capacity region of a the $|\mathcal{I}(n)|$ -user Gaussian multiaccess channel with power constraints p_l , $l \in \mathcal{I}(n)$ is given by the set of rate vectors that lie in the intersection of the constraints, i.e.,

$$\sum_{l \in \mathcal{V}(n)} r_l \leq \log \left(1 + \frac{\sum_{l \in \mathcal{V}(n)} g_{ll} p_l}{\sigma^2} \right) \tag{31}$$

for every subset $\mathcal{V}(n) \subseteq \mathcal{I}(n)$. Thus, we can rewrite (26) as

$$\begin{aligned}
 &\text{maximize} \quad \sum_{l \in \mathcal{I}(n)} \beta_l r_l \\
 &\text{subject to} \quad n \in \mathcal{N} \\
 &\quad \quad \quad \sum_{l \in \mathcal{V}(n)} r_l \leq \log \left(1 + \frac{\sum_{l \in \mathcal{V}(n)} g_{ll} p_l}{\sigma^2} \right), \\
 &\quad \quad \quad \mathcal{V}(n) \subseteq \mathcal{I}(n) \\
 &\quad \quad \quad 0 \leq p_l \leq p_{\text{tran}(l)}^{\max}, \quad l \in \mathcal{I}(n) \\
 &\quad \quad \quad p_l = 0, \quad l \notin \mathcal{I}(n),
 \end{aligned} \tag{32}$$

where the variables are n , p_l , and r_l . Again, the solution is obtained in two steps. First, we solve N independent subproblems (one subproblem for each possible receiving node $n \in \mathcal{N}$). Then, we select the solution of the subproblem with the largest objective value. The subproblem has the form

$$\begin{aligned}
 &\text{maximize} \quad \sum_{l \in \mathcal{I}(n)} \beta_l r_l \\
 &\text{subject to} \quad \sum_{l \in \mathcal{V}(n)} r_l \leq \log \left(1 + \frac{\sum_{l \in \mathcal{V}(n)} g_{ll} p_l}{\sigma^2} \right), \\
 &\quad \quad \quad \mathcal{V}(n) \subseteq \mathcal{I}(n) \\
 &\quad \quad \quad 0 \leq p_l \leq p_{\text{tran}(l)}^{\max}, \quad l \in \mathcal{I}(n),
 \end{aligned} \tag{33}$$

where the variables are r_l and p_l , $l \in \mathcal{I}(n)$. Problem (33) is equivalent to the weighted sum-rate maximization over the capacity region of the Gaussian multiaccess channel with $|\mathcal{I}(n)|$ users [56, Sec. 6]. The solution is readily obtained by considering the *polymatroid* structure of the capacity region [58, Lemma 3.2]. Again, we denote by $g^{(n)}$, $p_l^{(n)}$, and $r_l^{(n)}$ the optimal objective value and the optimal solution of (33), respectively. Thus, the solution of (33) can be written in closed form as $p_l^{(n)} = p_{\text{tran}(l)}^{\max}$ for all $l \in \mathcal{I}(n)$, and

$$r_{\pi_n(i)}^{(n)} = \log \left(1 + \frac{g_{\pi_n(i)\pi_n(i)} p_{\pi_n(i)}^{(n)}}{\sigma^2 + \sum_{j=i+1}^{|\mathcal{I}(n)|} g_{\pi_n(j)\pi_n(j)} p_{\pi_n(j)}^{(n)}} \right), \quad i \in \{1, \dots, |\mathcal{I}(n)|\}, \tag{34}$$

where $\pi_n = (\pi_n(1), \dots, \pi_n(|\mathcal{I}(n)|))$ is a permutation of the set of incoming links $\mathcal{I}(n)$ such that

$$\beta_{\pi_n(1)} \leq \beta_{\pi_n(2)} \leq \dots \leq \beta_{\pi_n(|\mathcal{I}(n)|)}. \tag{35}$$

We can, in fact, identify π_n as the SIC order at the receiving node $n \in \mathcal{N}$. Finally, the optimal solution of (32) can be expressed as

$$\begin{aligned} n^* &= \arg \max_{n \in \mathcal{N}} g^{(n)} \\ p_l^* &= \begin{cases} p_l^{(n^*)} & l \in \mathcal{I}(n^*) \\ 0 & \text{otherwise} \end{cases} \\ r_l^* &= \begin{cases} r_l^{(n^*)} & l \in \mathcal{I}(n^*) \\ 0 & \text{otherwise.} \end{cases} \end{aligned} \quad (36)$$

V. NUMERICAL RESULTS

In this section, we use the algorithms of the preceding sections to identify the solutions to the selected NUM problem and their properties to have insights into the NW design and provisioning methods. In particular, in every time slot t , the rate allocation at step 3 of the dynamic cross-layer control algorithm (i.e., *Algorithm 1*; see Section II) is obtained using the proposed RA algorithms described in Sections III and IV.

We assume a block-fading Rayleigh channel model, where the channel coefficients are constant during each time slot and independently change from one slot to another. The small-scale fading components of the channel gains are assumed to be independent and identically distributed over the time slots, links, and channels. Recall that we consider equal power spectral density for all receivers, i.e., $N_l = N_0$ for all $l \in \mathcal{L}$ and equal channel bandwidths, i.e., $W_c = W$ for all $c \in \mathcal{C}$. Furthermore, the maximum power constraint is assumed the same for all nodes, i.e., $p_n^{\max} = p_0^{\max}$ for all $n \in \mathcal{N}$ (independent of the number of channels C). For fair comparison between cases with different numbers of channels, we have assumed that the total available bandwidth is constant, regardless of C , i.e., $\sum_{c=1}^C W_c = W_{\text{tot}}$. In all our simulations, we have selected the total bandwidth to be normalized to 1, i.e., $W_{\text{tot}} = 1$ Hz.

To compare different algorithms, we consider the following two performance metrics: 1) *the average sum rate* $\sum_{n \in \mathcal{N}} \sum_{s \in \mathcal{S}_n} \bar{x}_n^s$ and 2) *the average NW congestion* $\sum_{n \in \mathcal{N}} \sum_{s=1}^S \bar{q}_n^s$. For each NW instance, the dynamic cross-layer control algorithm (i.e., *Algorithm 1*) is simulated for at least $T = 10000$ time slots, and the average rates \bar{x}_n^s and queue sizes \bar{q}_n^s are computed by averaging the last $t_0 = 3000$ time slots, i.e., $\bar{x}_n^s = 1/t_0 \sum_{t=T-t_0}^T x_n^s(t)$ and $\bar{q}_n^s = 1/t_0 \sum_{t=T-t_0}^T q_n^s(t)$. We assume that the average rates \bar{x}_n^s that correspond to all node-commodity pairs $(n, s)_{s \in \mathcal{S}_n}$, $n \in \mathcal{N}$, are subject to proportional fairness, and therefore, we select the utility functions $u_n^s(x) = \ln(x)$. In all the considered setups, we selected $V = 100$ [in (4)], and the parameters R_n^{\max} [in (4)] were chosen such that all the conditions in [4, Sec. III-D] were satisfied.

We start with a simple NW instance (see Section V-A), i.e., a bipartite NW, where there exist no self interferers (i.e., $\mathcal{A} = \emptyset$), and the proposed successive approximation algorithm (i.e., *Algorithm 2*; see Section III-B) is used in RA. The associate results show important consequences on upper layers due to the proposed successive approximation algorithm. We then con-

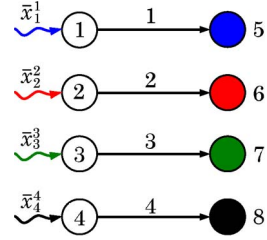


Fig. 3. Bipartite wireless NW with $N = 8$ nodes, $L = 4$ links, and $S = 4$ commodities.

sider more general NWs (see Section V-B) with the presence of self interferers (i.e., $\mathcal{A} \neq \emptyset$), where *Algorithm 3* (see Section III-D) is used in RA. Finally, we look at the MU receiver scenario, again using the same NW instance as in Section V-B. The associate results (see Section V-C) show impacts in the upper layer performance due to advanced receiver architecture.

A. Bipartite NWs: Receivers Perform Single-User Detection

A bipartite NW, as shown in Fig. 3, is considered. There are $N = 8$ nodes, $L = 4$ links, and $S = 4$ commodities. One distinct commodity exogenously arrives at every node n from the subset $\{1, 2, 3, 4\} \subseteq \mathcal{N}$. Without loss of generality, we assume that the nodes and commodities are labeled such that commodity i arrives at node i for any $i \in \{1, 2, 3, 4\}$. The destination nodes are specified by the following commodity-destination node pairs $(s, d_s) \in \{(1, 5), (2, 6), (3, 7), (4, 8)\}$.

The channel power gains between distinct nodes are given by

$$|h_{ijc}(t)|^2 = \mu^{|i-j|} c_{ijc}(t), \quad i, j \in \mathcal{L}, c \in \mathcal{C}, \quad (37)$$

where $c_{ijc}(t)$ are exponentially distributed independent random variables with unit mean used to model the Rayleigh small-scale fading, and the scalar $\mu \in [0, 1]$ is referred to as the interference coupling index, which parameterizes the interference between direct links. For example, if $\mu = 0$, transmissions of links are interference free. The interference between transmissions increases as the parameter μ grows. Similar channel gain models for bipartite NWs have also been used in [59]. Of course, this simple hypothetical model provides useful insights into the performance of the proposed algorithms in bipartite NWs (e.g., cellular NWs). We define the signal-to-noise ratio (SNR) operating point as

$$\text{SNR} = \frac{p_0^{\max}}{N_0 W_{\text{tot}}}. \quad (38)$$

Fig. 4 shows the dependence of the average sum rate, i.e., $\sum_{s=1}^4 \bar{x}_s^s$ in Fig. 4(a), and the average NW congestion, i.e., $\sum_{s=1}^4 \bar{q}_s^s$ in Fig. 4(b), on the interference coupling index μ for our proposed *Algorithm 2* and for the optimal baseline single-link activation (BLSLA) policy.¹¹ We consider the

¹¹A channel access policy where, during each time slot, only one link is activated in each channel, is called the BLSLA policy. Finding the optimal BLSLA policy that solves the RA subproblem (6) is a combinatorial problem with exponential complexity in C . Thus, it quickly becomes intractable, even for moderate values of C . However, for the case $C = 1$, the optimal BLSLA policy can easily be found, and it consists of activating, during each time slot, only the link that achieves the maximum weighted rate.

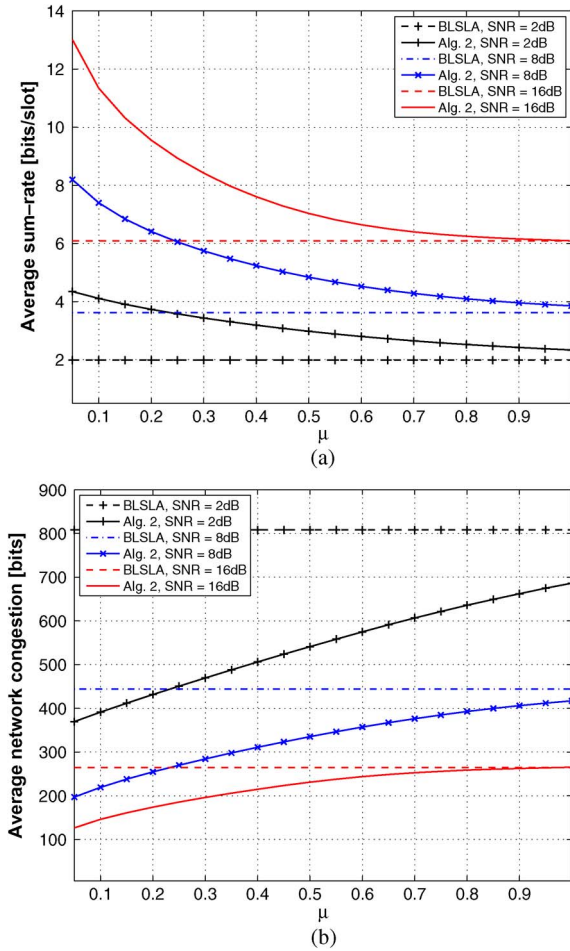


Fig. 4. Dependence of the average sum rate (top) and the average NW congestion (bottom) on the interference coupling index μ , where $C = 1$, and SNR = 2, 8, and 16 dB. (a) Average sum rate $\sum_{s=1}^4 \bar{x}_s^s$. (b) Average NW congestion $\sum_{s=1}^4 \bar{q}_s^s$.

single-channel case $C = 1$, which operates at three different SNR values 2, 8, and 16 dB. The initial power allocation \mathbf{P}_0 for *Algorithm 2* is chosen such that $[\mathbf{P}_0]_{l,1} = p_0^{\max}$, unless otherwise specified. Here, we can make several observations. First, the proposed *Algorithm 2* provides substantial gains both in the average sum rate and in the average NW congestion, particularly for small and medium values of the interference coupling index. The gains diminish as interference between direct links becomes significant. This behavior is intuitively expected, because for large SNR values, the BLSLA policy becomes optimal when the interference coupling index μ approaches 1. Note that, at small SNR values, the NW can still benefit from scheduling multiple links per slot, even for the case $\mu = 1$. This gain comes from the fact that the channels gains between interfering links are also affected by fading. Thus, links that experience low instantaneous interference levels can simultaneously be scheduled. Results suggest that, particularly for small and medium values of the interference coupling index, the proposed solution method yields designs that are far superior than the designs obtained by BLSLA.

Fig. 5(a) and (b) shows the dependence of the average sum rate and the average NW congestion on the number of iterations for *Algorithm 2*, respectively. We consider the single-channel

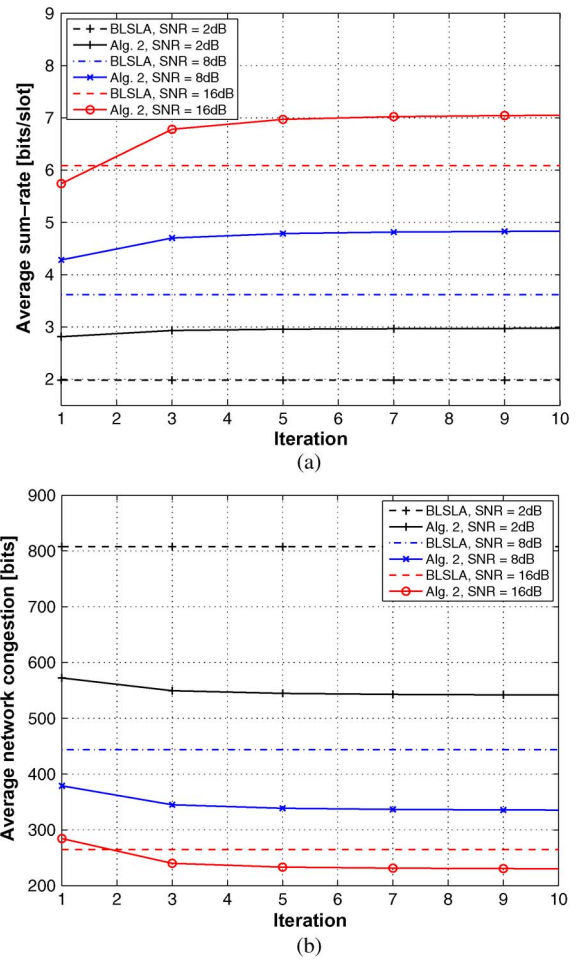


Fig. 5. Dependence of the average sum rate (top) and the average NW congestion (bottom) on the iteration, where $\mu = 0.5$, $C = 1$, and SNR = 2, 8, and 16 dB. (a) Average sum rate $\sum_{s=1}^4 \bar{x}_s^s$. (b) Average NW congestion $\sum_{s=1}^4 \bar{q}_s^s$.

case $C = 1$ with interference coupling index $\mu = 0.5$ and SNR values 2, 8, and 16 dB. To facilitate faster convergence, *Algorithm 2* is run without considering the trust region constraints.¹² As a reference, we consider the optimal BLSLA policy. Results show that the incremental benefits are very significant for the first few iterations and are marginal for the latter iterations. For example, in the case of SNR = 16 dB, when the numbers of iterations changes from 1 to 3, the improvement in the average sum rate is around 18.1%, whereas when it changes from 7 to 9, the improvement is around 0.30%. Therefore, by running *Algorithm 2* for few iterations (e.g., five iterations), we can yield performance levels that are almost indistinguishable from performance levels that would have been obtained by running *Algorithm 2* until it terminates (see the stopping criterion in step 3). This observation can be very useful in practice, because we can terminate *Algorithm 2* when the incremental improvements between consecutive iterations become substantially small.

Fig. 6(a) and (b) shows the dependence of the average sum rate and the average NW congestion, respectively, on the SNR

¹²To do this approach, we can simply set the parameter α in *Algorithm 2* to a very large positive number, e.g., $\alpha = 10^{100}$ [see (18)].

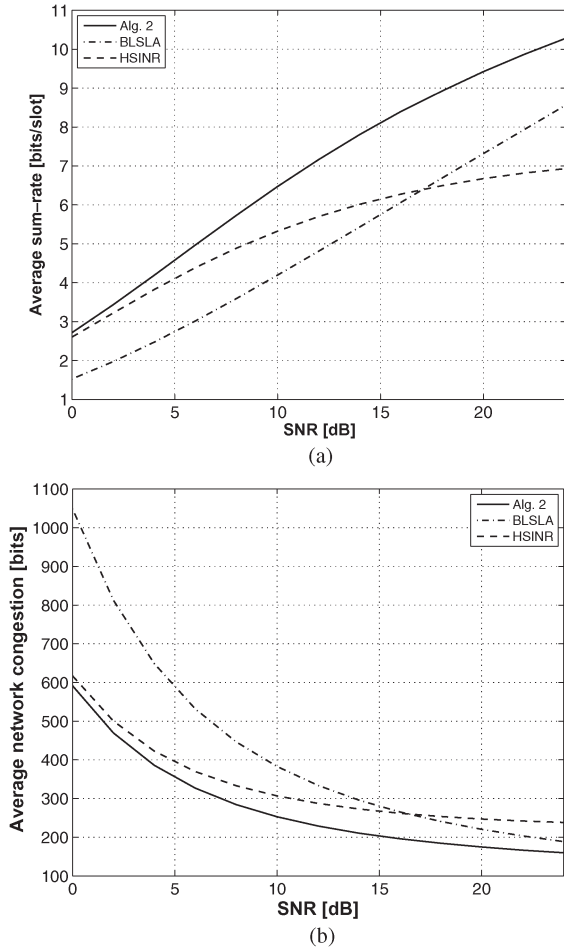


Fig. 6. Dependence of the average sum rate (top) and the average NW congestion (bottom) on the SNR, where $C = 1$, and $\mu = 0.3$. (a) Average sum rate $\sum_{s=1}^4 \bar{x}_s^s$. (b) Average NW congestion $\sum_{s=1}^4 \bar{q}_s^s$.

for *Algorithm 2* and the optimal BLSLA policy. We have considered the case where $C = 1$ and $\mu = 0.3$. For comparison, we also plot the results due to a commonly used HSINR approximation [33], where the achievable rates $\log(1 + \gamma_{lc})$ are approximated by $\log(\gamma_{lc})$.¹³ We should not confuse a HSINR with a high SNR, because they are fundamentally different, and a high SNR value does not ensure HSINR values in all links. Results show that, compared with other methods, RA based on *Algorithm 2* offers larger average sum rate and reduced average NW congestion. The relative gains of *Algorithm 2* are reduced compared with BLSLA at high SNR. For example, the relative gain offered by the proposed *Algorithm 2* in the average sum rate changes from 40% to 17% [see Fig. 6(a)], and the relative gain in the average NW congestion changes from 23% to 15% [see Fig. 6(b)] when the SNR value is increased from 16 to 24 dB, respectively. This observation is consistent with the fact that, at a high SNR, the optimal RA very likely has a BLSLA structure. As a result, at the optimal RA, different links correspond to different SINR regions, and therefore, the HSINR

¹³Here, the objective function of (11) is approximated by $\prod_{c \in \mathcal{C}} \prod_{l \in \mathcal{L}} \gamma_{lc}^{-\beta_l}$. Recall that γ_{lc} represents the SINR of link l in channel c , and β_l represents the differential backlog of link l . This results in a convex approximation (i.e., a GP) of (11).

approximation is, of course, unreasonable and suffers a large penalty, particularly at high SNR values. This poor performance is qualitatively consistent with intuition: the solution that is obtained by employing the HSINR approximation in RA must contain all nonzero entries (i.e., nonzero γ_{lc}) to drive the approximated objective (i.e., $\prod_{c \in \mathcal{C}} \prod_{l \in \mathcal{L}} \gamma_{lc}^{-\beta_l}$) into a nonzero value, and therefore never yields a solution of the form BLSLA.

Fig. 7(a) and (b) shows the dependence of the average sum rate and the average NW congestion on the numbers of channels C for *Algorithm 2*, respectively. We consider the case where SNR = 16 dB and $\mu = 0.3$, and the initial power allocation \mathbf{P}_0 for *Algorithm 2* is simply chosen such that $[\mathbf{P}_0]_{l,c} = p_0^{\max}/C$. The plots illustrate that increasing the number of channels will yield better performance in both the average sum rate and the average NW congestion (e.g., when the number of channels C changes from 1 to 8, the improvement in the average sum rate and the reduction in the average NW congestion is around 12% and 12.4%, respectively). Note that the benefits are solely achieved by opportunistically exploiting the available multi-channel diversity in the NW through the proposed *Algorithm 2*, without any supplementary bandwidth or power consumption. Moreover, the incremental benefits are very significant for small C . For example, when the number of channels C changes from 1 to 2, the improvement in the average sum rate is around 6%, whereas when C changes from 7 to 8, the improvement is around 0.25%. The plots give much insight into why multi-channel designs are important and beneficial compared with its single-channel counterpart.

B. Multihop NWs: Receivers Perform Single-User Detection

Two fully connected multihop wireless NW setups, as shown in Fig. 8, are considered. Each of the NW consist of four nodes (i.e., $N = 4$) and two commodities (i.e., $S = 2$), which exogenously arrive at the source nodes. In the case of the first NW setup shown in Fig. 8(a), commodity 1 exogenously arrives at node 1 and is intended for node 4, and commodity 2 exogenously arrives at node 4 and is intended for node 1. Nodes are located in a square grid such that the horizontal and the vertical distances between adjacent nodes are D_0 m. In the case of the second NW setup shown in Fig. 8(b), commodity 1 exogenously arrives at node 1 and is intended for node 2, and commodity 2 exogenously arrives at node 2 and is intended for node 3. Nodes are located such that three of them form an equilateral triangle and the fourth node is located at the center [see Fig. 8(b)]. It is assumed that the distance from the middle node to any other node is D_0 m.

We assume an exponential path loss model where the channel power gains $|h_{ijc}(t)|^2$ between distinct nodes are given by

$$|h_{ijc}(t)|^2 = \left(\frac{d_{ij}}{d_0}\right)^{-\eta} c_{ijc}(t), \quad (39)$$

where d_{ij} is the distance from the transmitter of link i to the receiver of link j , d_0 is the *far-field reference distance* [60], η is the path loss exponent, and $c_{ijc}(t)$ are exponentially distributed random variables with unit mean, independent over the time slots, links, and channels. The first term in (39) represents

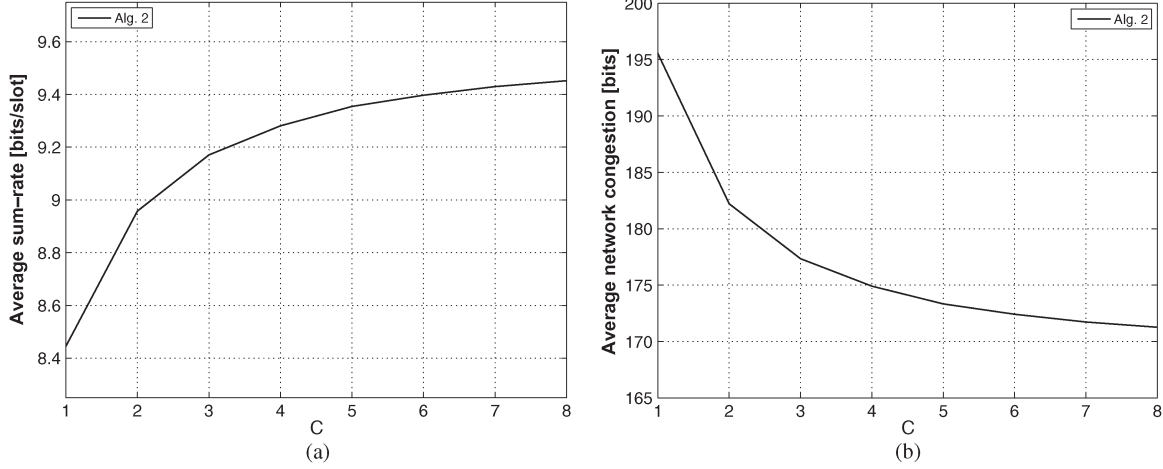


Fig. 7. Dependence of the average sum rate (left) and the average NW congestion (right) on the number of channels C , where $\text{SNR} = 16$ dB, and $\mu = 0.3$. (a) Average sum rate $\sum_{s=1}^4 \bar{x}_s^s$. (b) Average NW congestion $\sum_{s=1}^4 \bar{q}_s^s$.

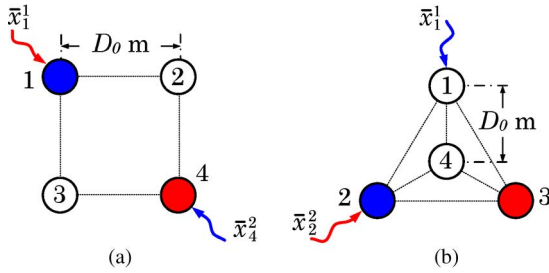


Fig. 8. (a) Multihop NW 1, $N = 4$, fully connected, and $S = 2$. (b) Multihop NW 2, $N = 4$, fully connected, and $S = 2$.

the path loss factor, and the second term models the Rayleigh small-scale fading. The SNR operating point is defined as

$$\text{SNR} = \frac{p_0^{\max}}{N_0 W_{\text{tot}}} \cdot \left(\frac{D_0}{d_0} \right)^{-\eta}. \quad (40)$$

In the following simulations, we set $D_0/d_0 = 10$ and $\eta = 4$.

Fig. 9 shows the dependence of the average NW layer sum rate on the SNR for the considered NW setups, where we use $C = 1$. As a benchmark, we first consider the branch-and-bound algorithm proposed in [27] to optimally solve the RA subproblem. Note that the optimality of the algorithm proposed in [27] is achieved at the expense of prohibitive computational complexity, even in the case of very small problem instances. We then consider the optimal BLSLA policy and *Algorithm 3* with the following two initialization methods: 1) uniform initialization and 2) BLSLA-based initialization. In the case of uniform initialization, the initial power allocation \mathbf{P}_0 is chosen such that $[\mathbf{P}_0]_{l^*,1} = p_0^{\max}/(|\mathcal{O}_{\text{tran}}(l)|)$. In the case of BLSLA based initialization the initial power allocation \mathbf{P}_0 is chosen such that $[\mathbf{P}_0]_{l^*,1} : [\mathbf{P}_0]_{j,1} = M : 1$ for all $j \in \mathcal{L}$, $j \neq l^*$, where l^* is the index of the active link obtained based on the optimal BLSLA policy, and $M \gg 1$ is a real number. For comparison, we also plot the results for *Algorithm 2* with uniform and BLSLA initializations.

Results show that the performance of *Algorithm 3* is very close to the optimal branch-and-bound algorithm. In particular, *Algorithm 3* with BLSLA initialization is almost indistinguish-

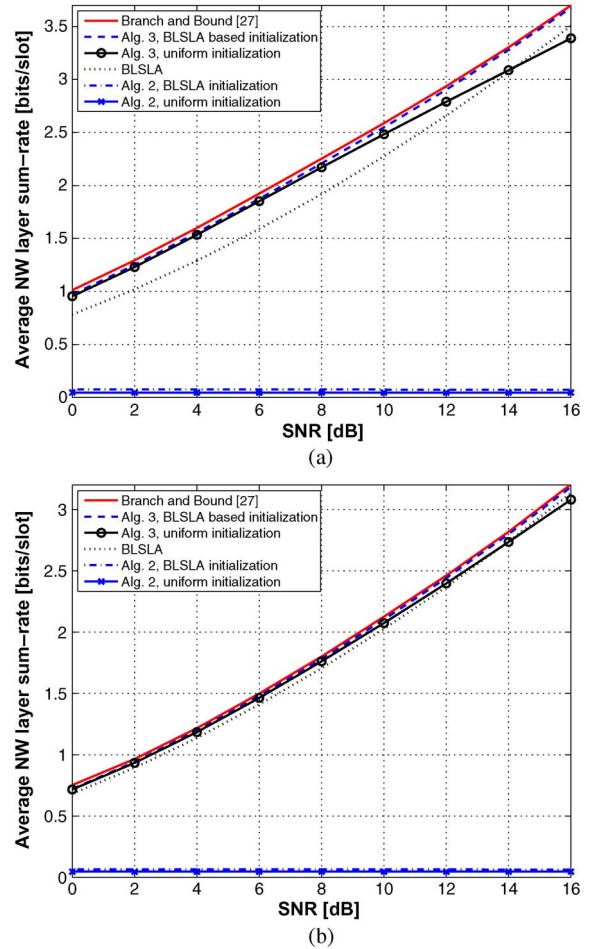
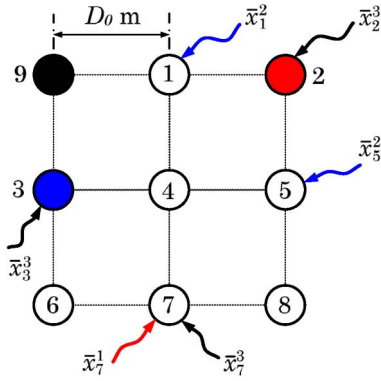


Fig. 9. (a) Dependence of the average NW-layer sum rate $\bar{x}_1^1 + \bar{x}_4^4$ on the SNR for NW 1. (b) Dependence of the average NW-layer sum rate $\bar{x}_1^1 + \bar{x}_2^2$ on the SNR for NW 2.

able from the optimal and is at least as good as the optimal BLSLA for all considered cases. In contrast, *Algorithm 3* with uniform initialization exhibits significant deviations from both the optimal branch-and-bound algorithm and BLSLA, particularly at high-SNR values. This behavior is not surprising, because *Algorithm 3* is a local method for the nonconvex RA

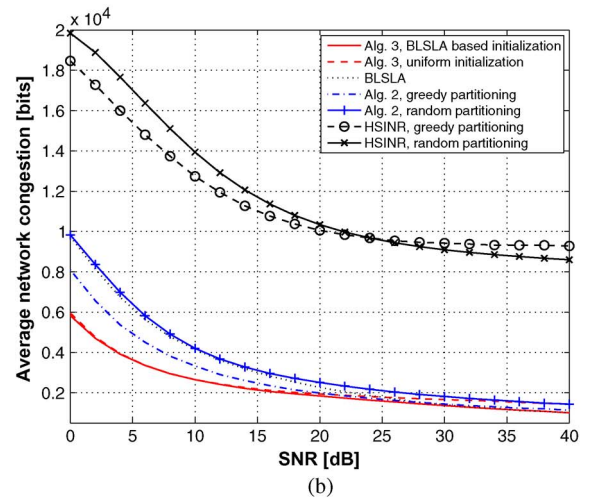
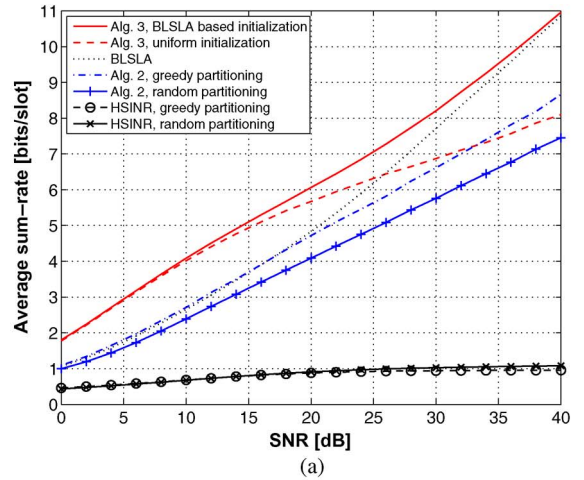
Fig. 10. Multihop wireless NW with $N = 9$ nodes and $S = 3$ commodities.TABLE I
NW COMMODITIES, DESTINATION NODES, AND SOURCE NODES

Commodity (s)	Destination node (d_s)	Source nodes
1	2	7
2	3	1, 5
3	9	2, 3, 7

subproblem (6). Therefore, the initialization point of the algorithm can influence the resulting solution [45, Sec. 1.4.1]. Nevertheless, a carefully selected initialization point can improve the performance of *Algorithm 3* very close to the optimal. For example, at high-SNR values, the performance of *Algorithm 3* with BLSLA initialization is almost identical to the optimal, whereas the performance with uniform initialization deviates a bit from the optimal. Note that, at low and moderate values of SNR, results due to *Algorithm 3* are not significantly affected by the initialization method. Results also convince that, in the presence of self interferers, *Algorithm 2* cannot perform well, and it can converge to a very bad suboptimal point, as pointed out in Section III-D. Therefore, although the computational complexity of *Algorithm 3* does not increase more than polynomially with the problem size, results show that *Algorithm 3* with a proper initialization performs close to the optimal.

Next, a larger NW, i.e., a fully connected multihop multicommodity wireless NW, as shown in Fig. 10, is considered. There are $N = 9$ nodes and $S = 3$ commodities. The commodities exogenously arrive at different nodes in the NW, as described in Table I. Thus, we have $\mathcal{S}_1 = \{2\}$, $\mathcal{S}_2 = \{3\}$, $\mathcal{S}_3 = \{3\}$, $\mathcal{S}_5 = \{2\}$, $\mathcal{S}_7 = \{1, 3\}$, and $\mathcal{S}_i = \emptyset$ for all $i \in \{4, 6, 8, 9\}$. The nodes are located in a rectangular grid such that the horizontal and vertical distances between adjacent nodes are D_0 m. The channel power gains between nodes are given by (39), and the SNR operating point is given by (40). Moreover, we set $D_0/d_0 = 10$ and $\eta = 4$.

Fig. 11(a) and (b) shows, respectively, the dependence of the average sum-rate and the average NW congestion on the SNR for several algorithms, where we use $C = 1$. First, we have considered the optimal BLSLA policy and *Algorithm 3* with the following two initialization methods: 1) uniform initialization and 2) BLSLA-based initialization (the same initializations that were used when plotting Fig. 9). For comparison, we also plot the results for the low complex approaches, where the set of nodes \mathcal{N} is first partitioned into two disjoint subsets (the set of transmitting nodes \mathcal{T} and the set of receiving nodes \mathcal{R}),

Fig. 11. Dependence of the average sum rate (top) and the average NW congestion (bottom) on the SNR, where $C = 1$. (a) Average sum rate $\sum_{n=1}^9 \sum_{s \in \mathcal{S}_n} \bar{x}_n^s$. (b) Average NW congestion $\sum_{n=1}^9 \sum_{s=1}^3 \bar{q}_n^s$.

and then, *Algorithm 2* and HSINR approximation are used in RA. The partitioning of the set of nodes \mathcal{N} into two disjoint subsets is performed using the following two simple methods: 1) random partitioning and 2) greedy partitioning based on differential backlogs. In random partitioning, each node is allocated either to \mathcal{T} or to \mathcal{R} with equal probabilities. Greedy partitioning is performed as follows. We start with an empty set of links $\tilde{\mathcal{L}} = \emptyset$. At each step, the link l^* from the set $\mathcal{L} \setminus \tilde{\mathcal{L}}$ with the largest differential backlog β_l (i.e., $l^* = \arg \max_{l \in \mathcal{L} \setminus \tilde{\mathcal{L}}} \beta_l$) is added to the set $\tilde{\mathcal{L}}$. Then, all links that are outgoing from $rec(l^*)$ and all links that are incoming to $tran(l^*)$ are deleted from $\tilde{\mathcal{L}}$. This procedure continues until there are no links left in $\mathcal{L} \setminus \tilde{\mathcal{L}}$. The sets \mathcal{T} and \mathcal{R} can be found as $\mathcal{T} = \{tran(l) | l \in \tilde{\mathcal{L}}\}$ and $\mathcal{R} = \{rec(l) | l \in \tilde{\mathcal{L}}\}$.

Based on Fig. 11, we make the following observations. First, *Algorithm 3* with BLSLA-based initialization yields better results than any other counterpart. In contrast, *Algorithm 3* with uniform initialization shows significant deviations from the BLSLA solution at high SNR, particularly in the terms of average sum rate [see Fig. 11(a)]. Moreover, it is important to again observe that, at low and moderate values of SNR, results due to *Algorithm 3* are not substantially affected by

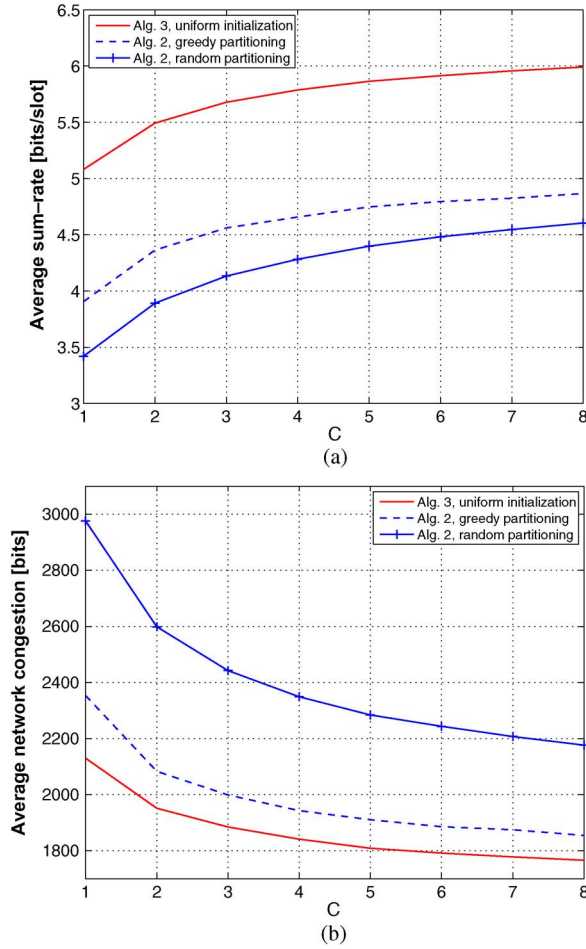


Fig. 12. Dependence of the average sum rate (top) and the average NW congestion (bottom) on the number of channels C , where SNR = 16 dB. (a) Average sum rate $\sum_{n=1}^9 \sum_{s \in \mathcal{S}_n} \bar{x}_n^s$. (b) Average NW congestion $\sum_{n=1}^9 \sum_{s=1}^3 \bar{q}_n^s$.

the initialization method. These observations are almost the same as the observations shown in Fig. 9. We also observe that *Algorithm 3* with a proper initialization can significantly outperform *Algorithm 2* in conjunction with either random or greedy partitioning. This elaborates the importance of gradual self-interference gain increments (i.e., step 4 of *Algorithm 3*) in finding a better RA compared to the direct application of *Algorithm 2* with a heuristic partitioning. In most cases, there is no advantage of using HSINR approximation. These observations are very useful in practice, because they illustrate that *Algorithm 3* often works well when initialized with a reasonable starting point (e.g., BLSLA-based initialization). In addition, we note that, even with a very simple initialization, e.g., uniform initialization, *Algorithm 3* yields substantial gains, particularly at small- and moderate-SNR values (e.g., 0–20 dB).

Fig. 12(a) and (b) shows the dependence of the average sum rate $\sum_{n=1}^9 \sum_{s \in \mathcal{S}_n} \bar{x}_n^s$ and the average NW congestion $\sum_{n=1}^9 \sum_{s=1}^3 \bar{q}_n^s$ on the numbers of channels C for *Algorithm 3*, respectively. We have considered the case where SNR = 16 dB and a uniform initialization for *Algorithm 3*, where the initial power allocation \mathbf{P}_0 is chosen such that $[\mathbf{P}_0]_{l,c} = p_0^{\max} / (C \cdot |\mathcal{O}_{\text{tran}(l)}|)$. For comparison, we also plot the results

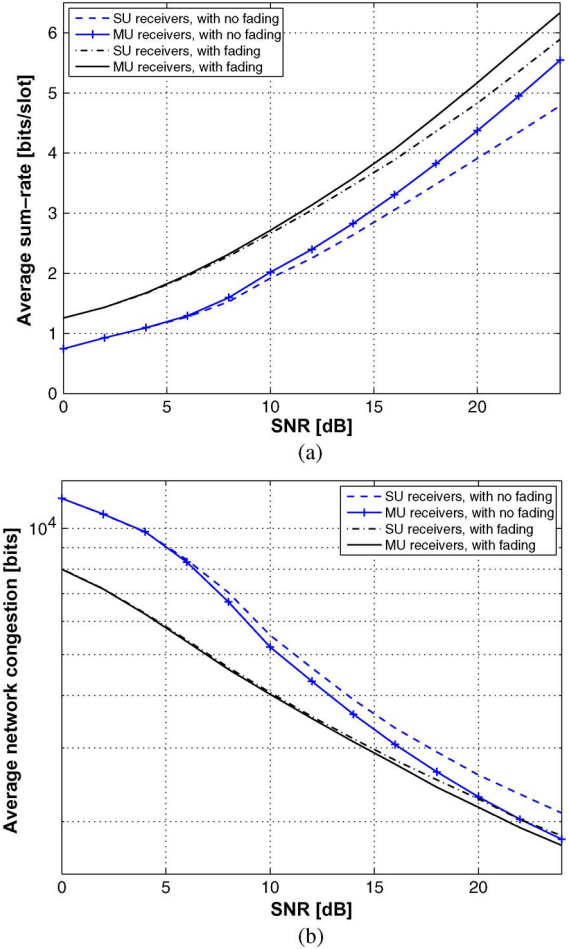


Fig. 13. Dependence of the average sum rate (top) and the average NW congestion (bottom) on the SNR, where $C = 1$. (a) Average sum rate $\sum_{n=1}^9 \sum_{s \in \mathcal{S}_n} \bar{x}_n^s$. (b) Average NW congestion $\sum_{n=1}^9 \sum_{s=1}^3 \bar{q}_n^s$.

for *Algorithm 2* with random and greedy partitioning of nodes \mathcal{N} . The results are consistent with our previous observations in Fig. 7, i.e., as the number of channels increases, better performance in both the average sum rate and the average NW congestion is achieved. These benefits are again obtained by opportunistically exploiting the available multichannel diversity in the NW through the proposed algorithms. Moreover, the results suggest that using *Algorithm 3* in the RA can very significantly increase the gains compared to RA based on simple extensions to *Algorithm 2*, which runs with either random or greedy partitioning of nodes. For example, the relative gains in the average sum rate are more than 23% [see Fig. 12(a)], and the relative gains in the average NW congestion are more than 4.7% [see Fig. 12(b)] over the range of interest: $C = 1$ to $C = 8$.

C. Multihop NWs: Single-Node Transmission Case and Receivers Perform MU Detection

The NW instance, assumptions, and simulation parameters are exactly the same as in Section V-B.

Fig. 13(a) and (b) shows, respectively, the dependence of the average sum rate $\sum_{n=1}^9 \sum_{s \in \mathcal{S}_n} \bar{x}_n^s$ and the average NW congestion $\sum_{n=1}^9 \sum_{s=1}^3 \bar{q}_n^s$ on the SNR for RA, where only one

node is allowed to transmit in each slot, and receivers perform MU detection. For illustration, we consider the single-channel case (i.e., $C = 1$). We also show the results for the nonfading case [i.e., by having $c_{ijc}(t) = 1$ in (39)] for comparison. Here, we can make several observations. Fading can significantly improve the overall performance in the average sum rate and the average NW congestion. This observation has an analogy with MU diversity in downlink fading channels [56, Sec. 6.6]. Intuition suggests that, when several links independently fade, at any time slot, there is a high probability that the resulting rate and power allocation yields a better schedule (see [8, Sec. 4.7]) compared with the nonfading case. There are significant advantages of having MU detection, particularly for high-SNR values. At low SNR, gains are marginal. Thus, MU detectors have a practical significance over SU detectors, particularly in the high-SINR regime. For example, in a fading environment, at SNR = 24 dB, we obtain around 7.5% increase in the average sum rate and 5% decrease in the average NW congestion. In a nonfading environment, MU detectors offer around 16% increase in the average sum rate and 13.5% decrease in the average NW congestion.

VI. CONCLUSION

We have considered the power and rate control problem in a wireless NW in conjunction with the next-hop routing/scheduling and flow control problem. Thus, although we have focused on the so-called RA problem, which is confined to the PHY/MAC layers, its formulation captures the interactions with the higher layers similar to the approach employed by Neely *et al.* for fairness and optimal stochastic control for heterogeneous NWs. The result is a cross-layer formulation. The problem, unfortunately, is NP-hard, and therefore, there are no polynomial-time algorithms for solve it. Our contribution has been to first consider a general access operation but with a relatively simple form of receivers structure (bank of match filters) and then to limit the access operation to a single node at a time (either transmitting or receiving) but allow for increased MU detector complexity at the receiver. In the first case, we offer a new optimization methodology based on homotopy methods and CGP solution methods. Numerical results showed that the proposed algorithms perform close to exponentially complex optimal solution methods. In addition, they are, of course, fast and can handle large-scale problems. In the second case, we obtain a complete solution and numerically illustrate the performance gain due to MU detector capability. The main benefit here is the simplicity of the proposed solution methods. As a result, these simple access protocols can potentially be useful in practical applications with more advanced communication systems.

APPENDIX A

DIRECT MONOMIAL APPROXIMATION

In this section, we derive a monomial approximation for the objective function of (11), which results in the same successive approximation steps as in *Algorithm 2*. We first prove the following lemma.

Lemma 2: Let $m(\gamma) = d \prod_{c \in \mathcal{C}} \prod_{l \in \mathcal{L}} \gamma_{lc}^{a_{lc}}$ be a monomial function [36] that is used to approximate the objective function (11), i.e., $f(\gamma) = \prod_{c \in \mathcal{C}} \prod_{l \in \mathcal{L}} (1 + \gamma_{lc})^{-\beta_l}$, near an arbitrary point $\{\hat{\gamma}_{lc} > 0\}_{l \in \mathcal{L}, c \in \mathcal{C}}$. The parameters d and a_{lc} of the best monomial local approximation are given by

$$a_{lc} = -\beta_l \hat{\gamma}_{lc} (1 + \hat{\gamma}_{lc})^{-1}, \quad d = f(\hat{\gamma}) \prod_{c \in \mathcal{C}} \prod_{l \in \mathcal{L}} \hat{\gamma}_{lc}^{-a_{lc}}, \quad (41)$$

where $\hat{\gamma}_{lc} = [\hat{\gamma}]_{l,c}$.

Proof: The monomial function m is the best local approximation of f near the point $\hat{\gamma}$ if (see [36])

$$m(\hat{\gamma}) = f(\hat{\gamma}), \quad \nabla m(\hat{\gamma}) = \nabla f(\hat{\gamma}). \quad (42)$$

By replacing the expressions of m and f in (42), we obtain the following system of equations:

$$\begin{cases} d \prod_{c \in \mathcal{C}} \prod_{l \in \mathcal{L}} \hat{\gamma}_{lc}^{a_{lc}} = f(\hat{\gamma}) \\ a_{lc} \hat{\gamma}_{lc}^{-1} d \prod_{c \in \mathcal{C}} \prod_{l \in \mathcal{L}} \hat{\gamma}_{lc}^{a_{lc}} = -\frac{\beta_l f(\hat{\gamma})}{(1 + \hat{\gamma}_{lc})} \quad c \in \mathcal{C}, l \in \mathcal{L} \end{cases}$$

the solution of which is given by (41). \blacksquare

By using the local approximation given by Lemma 2 in the objective function of (11) and ignoring the multiplicative constant d , which does not affect the problem solution, we obtain identical successive approximation steps as in *Algorithm 2*.

APPENDIX B

EXTENSION TO THE MULTICHANNEL SIC

In this section, we present the multichannel extension of the material presented in Section IV. The assumptions remain the same as in Section IV, i.e., at every node $n \in \mathcal{N}$ the transmitter independently performs superposition coding over its outgoing links $\mathcal{O}(n)$ in each channel $c \in \mathcal{C}$, and every receiving node $n \in \mathcal{N}$ performs SIC to decode the signals of incoming links $\mathcal{I}(n)$ in each channel $c \in \mathcal{C}$. In every channel $c \in \mathcal{C}$, the SIC receiver at every node $n \in \mathcal{N}$ has to decode and cancel out the signals of all its incoming links $\mathcal{I}(n)$ and any subset of the remaining links in its complement set $\mathcal{L} \setminus \mathcal{I}(n)$ to obtain the largest set of achievable rates. Let us denote the set of links that are decoded at the node n associated with each channel $c \in \mathcal{C}$ by $\mathcal{D}_c(n)$. Here, the set $\mathcal{D}_c(n) = \mathcal{I}(n) \cup \mathcal{U}_c(n)$ for some $\mathcal{U}_c(n) \subseteq \mathcal{L} \setminus \mathcal{I}(n)$. Furthermore, let $\mathcal{R}_c^{\text{SIC}}(\mathcal{D}_c(1), \dots, \mathcal{D}_c(N), p_{1c}^{\max}, \dots, p_{Nc}^{\max})$ denote the achievable rate region associated with channel $c \in \mathcal{C}$ for given $\mathcal{D}_c(1), \dots, \mathcal{D}_c(N)$ and the maximum node transmission power $p_{1c}^{\max}, \dots, p_{Nc}^{\max}$, where p_{nc}^{\max} is the maximum transmission power that is allocated to channel $c \in \mathcal{C}$ at node $n \in \mathcal{N}$. By taking the union of all possible combinations of sets $\mathcal{D}_c(1), \dots, \mathcal{D}_c(N)$, the achievable rate region that is associated with channel $c \in \mathcal{C}$ for a given maximum node transmission power $p_{1c}^{\max}, \dots, p_{Nc}^{\max}$ can be expressed as

$$\begin{aligned} & \mathcal{R}_c^{\text{SIC}}(p_{1c}^{\max}, \dots, p_{Nc}^{\max}) \\ &= \bigcup_{\mathcal{D}(1), \dots, \mathcal{D}(N) | \forall n \in \mathcal{N} \exists \mathcal{U}(n) \subseteq \mathcal{L} \setminus \mathcal{I}(n) \text{ s.t. } \mathcal{D}(n) = \mathcal{I}(n) \cup \mathcal{U}(n)} \mathcal{R}_c^{\text{SIC}}(\mathcal{D}(1), \dots, \mathcal{D}(N), p_{1c}^{\max}, \dots, p_{Nc}^{\max}). \end{aligned} \quad (43)$$

$$\mathcal{R}_c^{\text{SIC}}(\mathcal{D}_c(1), \dots, \mathcal{D}_c(N), p_{1c}^{\max}, \dots, p_{Nc}^{\max}) = \bigcup_{\pi_c} \left\{ (r_1, \dots, r_L) \left| \begin{array}{l} r_{\pi_{nc}(l)} \leq \log \left(1 + \frac{G_{\pi_{nc}(l)nc}(t)p_{\pi_{nc}(l)c}}{\sigma^2 + \sum_{j>l} G_{\pi_{nc}(j)nc}(t)p_{\pi_{nc}(j)c}} \right), \quad \forall (n, l) \text{ s.t. } n \in \mathcal{N}, l \in \{1, \dots, |\mathcal{D}_c(n)|\} \\ \sum_{l \in \mathcal{O}(n)} p_{lc} \leq p_{nc}^{\max}, \\ p_{lc} \geq 0, \end{array} \right. \right. \left. \left. \begin{array}{l} n \in \mathcal{N} \\ l \in \mathcal{L} \end{array} \right\} \quad (44)$$

Let $\pi_{nc} = (\pi_{nc}(1), \dots, \pi_{nc}(|\mathcal{D}_c(n)|))$ represent arbitrary permutations of the links in $\mathcal{D}_c(n)$, which describes the decoding and cancellation order at node n in channel c . The rate region $\mathcal{R}_c^{\text{SIC}}(\mathcal{D}_c(1), \dots, \mathcal{D}_c(N), p_{1c}^{\max}, \dots, p_{Nc}^{\max})$ is obtained by considering all possible combinations of decoding orders for all nodes, i.e., all possible $\prod_{n \in \mathcal{N}} (|\mathcal{D}_c(n)|!)$ combinations $\pi_c \triangleq \pi_{1c} \times \pi_{2c} \times \dots \times \pi_{Nc}$. Thus, the achievable rate region that is associated with channel $c \in \mathcal{C}$ for given $\mathcal{D}_c(1), \dots, \mathcal{D}_c(N)$ and the maximum node transmission power $p_{1c}^{\max}, \dots, p_{Nc}^{\max}$ can be expressed as in (44), shown at the top of the page,¹⁴ where $G_{lnc}, l \in \mathcal{L}, n \in \mathcal{N}, c \in \mathcal{C}$, represents the power gain from the transmitter of link l to the receiver at node n in channel c , and p_{lc} represents the power that is allocated for link l 's signal in channel c .

Therefore, by having superposition coding at the transmitters and SIC at the receivers, the achievable rate region for the interference channel can be expressed as

$$\mathcal{R}^{\text{SIC}}(p_1^{\max}, \dots, p_N^{\max}) = \left\{ (r_1, \dots, r_L) \left| \begin{array}{l} (r_1, \dots, r_L) \in \sum_{c \in \mathcal{C}} \mathcal{R}_c^{\text{SIC}}(p_{1c}^{\max}, \dots, p_{Nc}^{\max}) \\ \sum_{c \in \mathcal{C}} p_{nc} \leq p_n^{\max}, \quad n \in \mathcal{N} \\ p_{nc}^{\max} \geq 0, \quad n \in \mathcal{N}, l \in \mathcal{L} \end{array} \right. \right\}.$$

The RA subproblem at the third step of dynamic cross-layer control *Algorithm 1* is shown in (26). Finding the solution of this problem is extremely difficult, as aforementioned in the single-channel case, i.e., $C = 1$. However by limiting the access protocol so that only one node can transmit in all its outgoing links in each slot, the problem can be identified as a weighted sum-rate maximization over the capacity region of parallel Gaussian broadcast channels [57]. When only one node can receive from all its incoming links in each slot, the problem can be cast as a weighted sum-rate maximization over the capacity region of Gaussian vector multiaccess channel [61], [62, Sec. 6].

APPENDIX C BARRIER METHOD

In this section, we outline the basic steps in solving (28) using the *barrier method* [45, Sec. 11.3.1]. For notational simplicity, let us define $\sigma_{\rho_n(k)} = \sigma^2 / g_{\rho_n(k)\rho_n(k)}$ for $k = 1, \dots, |\mathcal{O}(n)|$ and $\sigma_{\rho_n(|\mathcal{O}(n)|+1)} = 0$. Furthermore, let \mathbf{a}_i be the i th column of the upper triangular matrix $\mathbf{A} \in \mathbb{R}_+^{|\mathcal{O}(n)| \times |\mathcal{O}(n)|}$, with all nonzero entries being equal to 1.

By characterizing the feasible set of rate allocation vector $\mathbf{r}_n = [r_{\rho_n(1)} \dots r_{\rho_n(|\mathcal{O}(n)|)}]^T$ [57, Sec. 3], (28) can equivalently be expressed as

$$\begin{aligned} & \text{maximize} && \sum_{l \in \mathcal{O}(n)} \beta_l r_l \\ & \text{subject to} && g_i(\mathbf{r}_n) \leq 0, \quad i = 1, \dots, |\mathcal{O}(n)| + 1, \end{aligned} \quad (45)$$

where the variables are \mathbf{r}_n . The function $g_i(\mathbf{r}_n)$ can compactly be expressed as

$$g_i(\mathbf{r}_n) = \begin{cases} -\mathbf{e}_i^T \mathbf{r}_n & 1 \leq i \leq |\mathcal{O}(n)| \\ \sum_{j=1}^{|\mathcal{O}(n)|} b_n(j) e^{\mathbf{a}_j^T \mathbf{r}_n - \sigma_{\rho_n(1)} - p_n^{\max}} & i = |\mathcal{O}(n)| + 1, \end{cases}$$

where $b_n(j) = \sigma_{\rho_n(j)} - \sigma_{\rho_n(j+1)}$. Problem (45) is a convex optimization problem [45] and can therefore efficiently be solved. Note that, given any feasible \mathbf{r}_n , the corresponding power variables $p_{\rho_n(k)}, k = 1, \dots, |\mathcal{O}(n)|$ are given by [57]

$$p_{\rho_n(k)} = (e^{r_{\rho_n(k)}} - 1) \sum_{i \geq k} b_n(i) e^{\sum_{k < j \leq i} r_{\rho_n(j)}}.$$

The *barrier method* [45, Sec. 11.3.1] can be used to solve (45). The gradient and the Hessian of the function $g_i(\mathbf{r}_n)$ are given by

$$\begin{aligned} \nabla g_i(\mathbf{r}_n) &= \begin{cases} -\mathbf{e}_i & 1 \leq i \leq |\mathcal{O}(n)| \\ \sum_{j=1}^{|\mathcal{O}(n)|} b_n(j) e^{\mathbf{a}_j^T \mathbf{r}_n} \mathbf{a}_j & i = |\mathcal{O}(n)| + 1 \end{cases} \\ \nabla^2 g_i(\mathbf{r}_n) &= \begin{cases} \mathbf{0} & 1 \leq i \leq |\mathcal{O}(n)| \\ \sum_{j=1}^{|\mathcal{O}(n)|} b_n(j) e^{\mathbf{a}_j^T \mathbf{r}_n} \mathbf{a}_j \mathbf{a}_j^T & i = |\mathcal{O}(n)| + 1. \end{cases} \end{aligned}$$

The aforementioned expressions are used to evaluate the gradient and the Hessian of the logarithmic barrier function [45, Sec. 11.2.1].

REFERENCES

- [1] F. P. Kelly, A. Maulloo, and D. Tan, "Rate control for communication networks: Shadow prices, proportional fairness, and stability," *J. Opt. Res. Soc.*, vol. 49, no. 3, pp. 237–252, Mar. 1998.
- [2] F. P. Kelly, "Charging and rate control for elastic traffic," *Eur. Trans. Telecommun.*, vol. 8, no. 1, pp. 33–37, Jan. 1997.
- [3] X. Lin and N. B. Shroff, "Joint rate control and scheduling in multihop wireless networks," in *Proc. IEEE Int. Conf. Decision Control*, Atlantis, The Bahamas, Dec. 14–17, 2004, vol. 5, pp. 1484–1489.
- [4] M. J. Neely, E. Modiano, and C. Li, "Fairness and optimal stochastic control for heterogeneous networks," *IEEE/ACM Trans. Netw.*, vol. 16, no. 2, pp. 396–409, Apr. 2008.

¹⁴Note that we assume equal channel bandwidths for all $c \in \mathcal{C}$.

- [5] A. L. Stolyar, "Maximizing queuing network utility subject to stability: Greedy primal-dual algorithm," *Queueing Syst.*, vol. 50, no. 4, pp. 401–457, Aug. 2005.
- [6] A. Eryilmaz and R. Srikant, "Fair resource allocation in wireless networks using queue-length-based scheduling and congestion control," *IEEE/ACM Trans. Netw.*, vol. 15, no. 6, pp. 1333–1344, Dec. 2007.
- [7] A. Eryilmaz and R. Srikant, "Joint congestion control, routing and MAC for stability and fairness in wireless networks," *IEEE J. Sel. Areas Commun.*, vol. 24, no. 8, pp. 1514–1524, Aug. 2006.
- [8] L. Georgiadis, M. J. Neely, and L. Tassiulas, "Resource allocation and cross-layer control in wireless networks," *Found. Trends Netw.*, vol. 1, no. 1, pp. 1–144, Apr. 2006.
- [9] M. J. Neely, "Dynamic power allocation and routing for satellite and wireless networks with time varying channels," Ph.D. dissertation, Dept. Elect. Eng. Comput. Sci., Mass. Inst. Technol., Cambridge, MA, 2003.
- [10] X. Lin, N. B. Shroff, and R. Srikant, "A tutorial on cross-layer optimization in wireless networks," *IEEE J. Sel. Areas Commun.*, vol. 24, no. 8, pp. 1452–1463, Aug. 2006.
- [11] Y. Yi and M. Chiang, "Stochastic network utility maximization: A tribute to Kelly's paper published in this journal a decade ago," *Eur. Trans. Telecommun.*, vol. 19, no. 4, pp. 421–442, Jun. 2008.
- [12] L. Tassiulas and A. Ephremides, "Stability properties of constrained queueing systems and scheduling policies for maximum throughput in multihop radio networks," *IEEE Trans. Autom. Control*, vol. 37, no. 12, pp. 1936–1948, Dec. 1992.
- [13] L. Tassiulas and A. Ephremides, "Dynamic server allocation to parallel queues with randomly varying connectivity," *IEEE Trans. Inf. Theory*, vol. 39, no. 2, pp. 466–478, Mar. 1993.
- [14] M. J. Neely, E. Modiano, and C. E. Rohrs, "Dynamic power allocation and routing for time-varying wireless networks," *IEEE J. Sel. Areas Commun.*, vol. 23, no. 1, pp. 89–103, Jan. 2005.
- [15] A. L. Stolyar, "Maxweight scheduling in a generalized switch: State space collapse and workload minimization in heavy traffic," *Ann. Appl. Probab.*, vol. 14, no. 1, pp. 1–53, 2004.
- [16] Z. Q. Luo and W. Yu, "An introduction to convex optimization for communications and signal processing," *IEEE J. Sel. Areas Commun.*, vol. 24, no. 8, pp. 1426–1438, Aug. 2006.
- [17] Z. Luo and S. Zhang, "Dynamic spectrum management: Complexity and duality," *IEEE J. Sel. Areas Commun.*, vol. 2, no. 1, pp. 57–73, Feb. 2008.
- [18] R. Horst, P. Pardalos, and N. Thoai, *Introduction to Global Optimization*, 2nd ed. Dordrecht, The Netherlands: Kluwer, 2000.
- [19] C. Audet, P. Hansen, and G. Savard, Eds., *Essays and Surveys in Global Optimization*. New York: Springer-Verlag, 2005.
- [20] S. Boyd, *Branch-and-bound methods*, 2007. [Online]. Available: http://www.stanford.edu/class/ee364b/lectures/bb_slides.pdf
- [21] E. L. Allgower and K. Georg, *Introduction to Numerical Continuation Methods*. Philadelphia, PA: SIAM, 2003.
- [22] M. Avrieli and A. C. Williams, "Complementary geometric programming," *SIAM J. Appl. Math.*, vol. 19, no. 1, pp. 125–141, Jul. 1970.
- [23] R. Cendrillon, W. Yu, M. Moonen, J. Verlinden, and T. Bostoen, "Optimal multiuser spectrum balancing for digital subscriber lines," *IEEE Trans. Commun.*, vol. 54, no. 5, pp. 922–933, May 2006.
- [24] P. Tsiaflakis, J. Vangorp, M. Moonen, and J. Verlinden, "A low-complexity optimal spectrum-balancing algorithm for digital subscriber lines," *Signal Process.*, vol. 87, no. 7, pp. 1735–1753, Jul. 2007.
- [25] Y. Xu, T. Le-Ngoc, and S. Panigrahi, "Global concave minimization for optimal spectrum balancing in multiuser DSL networks," *IEEE Trans. Signal Process.*, vol. 56, no. 7, pp. 2875–2885, Jul. 2008.
- [26] L. Qian, Y. J. Zhang, and J. Huang, "MAPEL: Achieving global optimality for a nonconvex wireless power control problem," *IEEE Trans. Wireless Commun.*, vol. 8, no. 3, pp. 1553–1563, Mar. 2009.
- [27] P. C. Weeraddana, M. Codreanu, M. Latva-aho, and A. Ephremides, "Weighted sum-rate maximization for a set of interfering links via branch and bound," *IEEE Trans. Signal Process.*, 2011, to be published. [Online]. Available: http://www.ee.oulu.fi/~chathu/IEEE_TSP_Minor_2011.pdf
- [28] M. Z. Win and R. A. Scholtz, "Ultrawide bandwidth time-hopping spread-spectrum impulse radio for wireless multiple-access communications," *IEEE Trans. Commun.*, vol. 48, no. 4, pp. 679–691, Apr. 2000.
- [29] B. Radunovic and J. L. Boudec, "Optimal power control, scheduling, and routing in UWB networks," *IEEE J. Sel. Areas Commun.*, vol. 22, no. 7, pp. 1252–1270, Sep. 2004.
- [30] Y. Souilmi, R. Knopp, and G. Caire, "Coding strategies for UWB interference-limited peer-to-peer networks," in *Proc. Int. Symp. Model. Optim. Mobile, Ad Hoc Wireless Netw.*, Sophia-Antipolis, France, Mar. 3–5, 2003.
- [31] B. Radunovic and J. Le Boudec, "Power control is not required for wireless networks in the linear regime," in *Proc. WOWMOM*, Taormina, Italy, Jun. 13–16, 2005, vol. 5, pp. 417–427.
- [32] R. L. Cruz and A. V. Santhanam, "Optimal routing, link scheduling and power control in multihop wireless networks," in *Proc. IEEE INFOCOM*, San Diego, CA, Apr. 2003, vol. 1, pp. 702–711.
- [33] M. Chiang, "Balancing transport and physical layers in wireless multihop networks: Jointly optimal congestion control and power control," *IEEE J. Sel. Areas Commun.*, vol. 23, no. 1, pp. 104–116, Jan. 2005.
- [34] D. C. O'Neill, D. Julian, and S. Boyd, "Optimal routes and flows in congestion constrained ad hoc networks," in *Proc. IEEE Veh. Technol. Conf.*, Los Angeles, CA, Sep. 26–29, 2004, pp. 702–711.
- [35] D. Julian, M. Chiang, D. O'Neill, and S. Boyd, "QoS and fairness constrained convex optimization of resource allocation for wireless cellular and ad hoc networks," in *Proc. IEEE INFOCOM*, New York, Jun. 2002, vol. 2, pp. 477–486.
- [36] S. Boyd, S. J. Kim, L. Vandenberghe, and A. Hassibi, "A tutorial on geometric programming," *Optim. Eng.*, vol. 8, no. 1, pp. 67–127, 2007.
- [37] M. Chiang, "Geometric programming for communication systems," *Found. Trends Commun. Inf. Theory*, vol. 2, no. 1/2, pp. 1–154, Jul. 2005.
- [38] M. Chiang, C. W. Tan, D. P. Palomar, D. O'Neill, and D. Julian, "Power control by geometric programming," *IEEE Trans. Wireless Commun.*, vol. 6, no. 7, pp. 2640–2651, Jul. 2007.
- [39] M. Codreanu, A. Tolli, M. Juntti, and M. Latva-aho, "Joint design of Tx–Rx beamformers in MIMO downlink channel," *IEEE Trans. Signal Process.*, vol. 55, no. 9, pp. 4639–4655, Sep. 2007.
- [40] A. Tölli, M. Codreanu, and M. Juntti, "Cooperative MIMO-OFDM cellular system with soft handover between distributed base station antennas," *IEEE Trans. Wireless Commun.*, vol. 7, no. 4, pp. 1428–1440, Apr. 2008.
- [41] S. A. Borbash and A. Ephremides, "The feasibility of matchings in a wireless network," *IEEE Trans. Inf. Theory*, vol. 52, no. 6, pp. 2749–2755, Jun. 2006.
- [42] S. A. Borbash and A. Ephremides, "Wireless link scheduling with power control and SINR constraints," *IEEE Trans. Inf. Theory*, vol. 52, no. 11, pp. 5106–5111, Nov. 2006.
- [43] B. Hajek and G. Sasaki, "Link scheduling in polynomial time," *IEEE Trans. Inf. Theory*, vol. 34, no. 5, pp. 910–917, Sep. 1988.
- [44] B. R. Marks and G. P. Wright, "A general inner approximation algorithm for nonconvex mathematical programs," *Oper. Res.*, vol. 26, no. 4, pp. 681–683, Jul./Aug. 1978.
- [45] S. Boyd and L. Vandenberghe, *Convex Optimization*. Cambridge, U.K.: Cambridge Univ. Press, 2004.
- [46] S. Boyd, *Sequential Convex Programming*, 2007. [Online]. Available: http://www.stanford.edu/class/ee364b/lectures/seq_slides.pdf
- [47] X. Lin and N. B. Shroff, *Joint Rate Control and Scheduling in Multihop Wireless Networks*, Purdue Univ., West Lafayette, IN. [Online]. Available: <http://cobweb.ecn.purdue.edu/~linx/papers.html>
- [48] X. Wu and R. Srikant, "Regulated maximal matching: A distributed scheduling algorithm for multihop wireless networks with node-exclusive spectrum sharing," in *Proc. IEEE Conf. Decision Control, Eur. Control Conf.*, Seville, Spain, Dec. 12–15, 2005, pp. 5342–5347.
- [49] M. Cao, X. Wang, S. Kim, and M. Madhian, "Multihop wireless backhaul networks: A cross-layer design paradigm," *IEEE J. Sel. Areas Commun.*, vol. 25, no. 4, pp. 738–748, May 2007.
- [50] M. Kodialam and T. Nandagopal, "Characterizing achievable rates in multihop wireless mesh networks with orthogonal channels," *IEEE/ACM Trans. Netw.*, vol. 13, no. 4, pp. 868–880, Aug. 2005.
- [51] Y. Shi and Y. T. Hou, "A distributed optimization algorithm for multihop cognitive radio networks," in *Proc. IEEE INFOCOM*, Phoenix, AZ, Apr. 13–18, 2008, pp. 1292–1300.
- [52] M. Cao, V. Raghunathan, S. Hanly, V. Sharma, and P. R. Kumar, "Power control and transmission scheduling for network utility maximization in wireless networks," in *Proc. IEEE Int. Conf. Decision Control*, New Orleans, LA, Dec. 12–14, 2007, pp. 5215–5221.
- [53] D. E. Barreto and S. S. Chiu, "Decomposition methods for cross-layer optimization in wireless networks," in *Proc. IEEE Wireless Commun. Netw. Conf.*, Kowloon, Hong Kong, Mar. 11–15, 2007, pp. 270–275.
- [54] M. Kojima, N. Megiddo, and T. Noma, "Homotopy continuation methods for nonlinear complementarity problems," *Math. Oper. Res.*, vol. 16, no. 4, pp. 754–774, Nov. 1991.
- [55] Y. Nesterov and A. Nemirovsky, *Interior-Point Polynomial Algorithms in Convex Programming*. Philadelphia, PA: SIAM, 1994.
- [56] D. Tse and P. Viswanath, *Fundamentals of Wireless Communication*. Cambridge, U.K.: Cambridge Univ. Press, 2005.
- [57] D. N. Tse, "Optimal power allocation over parallel Gaussian broadcast channels," in *Proc. Int. Symp. Inf. Theory*, Ulm, Germany, 1997.

- [58] D. N. Tse and S. V. Hanly, "Multiaccess fading channels—Part I: Poly-matroid structure, optimal resource allocation and throughput capacities," *IEEE Trans. Inf. Theory*, vol. 44, no. 7, pp. 2796–2815, Nov. 1998.
- [59] A. Pantelidou and A. Ephremides, "A cross-layer view of optimal scheduling," *IEEE Trans. Inf. Theory*, vol. 56, no. 11, pp. 5568–5580, Nov. 2010.
- [60] A. Kumar, D. Manjunath, and J. Kuri, *Wireless Networking*. Burlington, MA: Elsevier, 2008.
- [61] W. Yu, W. Rhee, S. Boyd, and J. Cioffi, "Iterative water-filling for Gaussian vector multiple-access channels," *IEEE Trans. Inf. Theory*, vol. 50, no. 1, pp. 145–152, Jan. 2004.
- [62] S. A. Jafar, "Fundamental capacity limits of multiple antenna wireless systems," Ph.D. dissertation, Stanford Univ., Stanford, CA, Aug. 2003.



Pradeep Chaturanga Weeraddana (S'08) received the B.Sc. (first-class honors) degree in electronics and telecommunication engineering from the University of Moratuwa, Moratuwa, Sri Lanka, in 2004 and the M.Eng. degree in telecommunications from the Asian Institute of Technology, Bangkok, Thailand, in 2007. He is currently working toward the Ph.D. degree with the Centre for Wireless Communications, Department of Electrical Engineering, University of Oulu, Oulu, Finland.

His research interests include applications of optimization techniques for signal processing and wireless communications.



Marian Codreanu (S'02–M'07) received the M.S. degree from the University Politehnica of Bucharest, Bucharest, Romania, in 1998 and the Ph.D. degree from the University of Oulu, Oulu, Finland, in 2007.

From 1998 to 2002, he was a Teaching Assistant with the Department of Telecommunications, University Politehnica of Bucharest. In 2002, he joined the Centre for Wireless Communications, Department of Electrical Engineering, University of Oulu, where he is currently a Senior Research Fellow.

In 2008, he was a Visiting Postdoctoral Researcher with the University of Maryland, College Park. His research interests include optimization, information theory, and signal processing for wireless communication systems and networks.

Dr. Codreanu was a Cochair of the Technical Program Committee of the First Nordic Workshop on Cross-Layer Optimization in Wireless Networks in 2010 and the Second Nordic Workshop on System and Network Optimization for Wireless in 2011. He received the Best Doctoral Thesis Prize within all technical sciences in Finland in 2007.



Matti Latva-aho (S'96–M'98–SM'06) was born in Kuivaniemi, Finland, in 1968. He received the M.Sc., Lic.Tech., and Dr. Tech (Hons.) degrees in electrical engineering from the University of Oulu, Oulu, Finland, in 1992, 1996, and 1998, respectively.

From 1992 to 1993, he was a Research Engineer with Nokia Mobile Phones, Oulu. From 1994 to 1998, he was a Research Scientist with the Telecommunication Laboratory and the Centre for Wireless Communications, Department of Electrical Engineering, University of Oulu, where he is currently

the Head of the Telecommunication Laboratory and a Professor of digital transmission techniques. From 1998 to 2006, he was the Director of the Centre for Wireless Communications. He has published 200 conference proceedings and journal papers in wireless communications. His research interests include mobile broadband wireless communication systems.



Anthony Ephremides (S'68–M'71–SM'77–F'84) received the Ph.D. degree in electrical engineering from Princeton University, Princeton, NJ, in 1971.

Since 1980, he has been the President of Pontos, Inc. He is currently the Cynthia Kim Professor of information technology with the Department of Electrical and Computer Engineering, University of Maryland, College Park, where he holds a joint appointment with the Institute for Systems Research, of which he was among the Founding Members in 1986. He has held various visiting positions with

other institutions, including the Massachusetts Institute of Technology; the University of California at Berkeley; the Swiss Federal Institute of Technology, Zurich, Switzerland; and the National Institute for Research in Computer Science and Control, France. In 1991, he cofounded and codirected the National Aeronautics and Space Administration-funded Center on Satellite and Hybrid Communication Networks. He is the author of several hundred papers and conference proceedings and the holder of several patents. His research interests include communication systems, networks, and all related disciplines, e.g., information theory, control and optimization, satellite systems, queuing models, and signal processing, particularly wireless networks and energy efficient systems.

Dr. Ephremides was the President of the IEEE Information Theory Society in 1987 and a Member of the IEEE Board of Directors in 1989 and 1990. He has been the General Chair or the Technical Program Chair of several technical conferences, including the IEEE Information Theory Symposium in 1991, 2000, and 2011, the IEEE Conference on Decision and Control in 1986, the Association for Computing Machinery (ACM) Mobihoc in 2003, and the IEEE Infocom in 1999. He has served on the Editorial Board of numerous journals and was the Founding Director of the Fairchild Scholars and Doctoral Fellows Program, which is a university–industry partnership, from 1981 to 1985. He received the IEEE Donald E. Fink Prize Paper Award in 1991 and the first ACM Achievement Award for Contributions to Wireless Networking in 1996, as well as the 2000 Fred W. Ellersick Military Communications Conference Best Paper Award, the IEEE Third Millennium Medal, the 2000 Outstanding Systems Engineering Faculty Award from the Institute for Systems Research, the Kirwan Faculty Research and Scholarship Prize from the University of Maryland in 2001, and a few other official recognitions of his work. He also received the 2006 Aaron Wyner Award for Exceptional Service and Leadership from the IEEE Information Theory Society.